Università degli Studi di Padova

Dipartimento di Psicologia dello Sviluppo e della Socializzazione

SCUOLA DI DOTTORATO DI RICERCA IN SCIENZE PSICOLOGICHE

INDIRIZZO DI SCIENZE COGNITIVE

XXV CICLO

Combining DTI and fMRI to investigate language lateralisation

Direttore della Scuola: Ch.ma Prof.ssa Clara Casco

Coordinatore d'indirizzo: Ch.ma Prof.ssa Francesca Peressotti

Supervisore: Ch.mo Prof. Giuseppe Sartori

Dottorando: Alessio Barsaglini

Table of Contents

ABSTRACT

Hemispheric lateralisation in the human brain has been a focus of interest in different fields of neurosciences since a long time (Galaburda, LeMay, Kemper, & Geschwind, 1978; Rubino, 1970).

One of the most studied and earliest observed lateralised brain functions is language. Reported in the nineteenth by the French physician and anatomist Paul Broca (1861) and by the German anatomist and neuropathologist Carl Wernicke (1874), language was found to be more impaired following tumours or strokes in the left hemisphere.

In recent years, a number of studies have employed diffusion tensor imaging (DTI) to characterize left hemisphere language-related white matter pathways (Barrick, Lawes, Mackay, & Clark, 2007; Bernal & Altman, 2010; Catani et al., 2007; Glasser & Rilling, 2008; Hagmann et al., 2006; Parker et al., 2005; Propper et al., 2010; Upadhyay, Hallock, Ducros, Kim, & Ronen, 2008; Vernooij et al., 2007). In addition, lesion and fMRI studies in healthy subjects have indicated that speech comprehension and production are lateralised to the left brain hemisphere (A. U. Turken & Dronkers, 2011).

The main aim of the present doctoral work is to better delineate the relationship between anatomical and functional correlates of hemispheric dominance in the perisylvian language network. To this purpose a multi-modal neuroimaging approach including DTI and fMRI on a population of 23 healthy individuals was applied.

In the first study, a virtual in vivo interactive dissection of the three subcomponents of the arcuate fasciculus was carried out and measures of perisylvian white matter integrity were derived from tract-specific dissection. Consistently with previous studies (Barrick, et al., 2007; Buchel et al., 2004; Catani, et al., 2007; Powell et al., 2006), a significant leftward asymmetry in the fractional anysotropy (FA) value of the long direct segment of the arcuate fasciculus (AF) has been found. In addition, I found another significant leftward lateralisation in the streamlines (SL) of the posterior segment and a rightward distribution of the SL index of the anterior segment of the AF. Finally, I found no evidence of a significant relationship between the leftward lateralisation indeces and any measures of language and verbal memory performance in my group.

In the second study, I implemented functional connectivity analysis to test whether leftward lateralisation of connectivity indeces between perisylvian regions can be observed in individuals performing a language-related task. The main finding of the functional connectivity analysis is a significant rightward lateralisation (left, 0.347 ± 0.183; right, 0.493 ± 0.228; P = 0.037) in the anterior connection, between the the inferior frontal gyrus (IFG) and the inferior parietal lobe (IPG).

In the third study, I combined DTI and fMRI data to examine whether a significant relationship is present between these measures of perisylvian connectivity and it significantly differs between hemispheres. The correlation analysis demonstrated significant negative relations between the mean FA values in the long segment of the AF and the strength of inter-regional coupling between the IFG and the middle temporal gyrus (MTG) in the left hemisphere, and between the mean FA values in the anterior segment of the AF and the strength of regional coupling between IFG

and IPL in the right hemisphere. Finally, there were no significant correlations between laterality indices estimated on FA and functional connectivity values.

SOMMARIO

La lateralizzazione emisferica cerebrale è un grande tema d'interesse nelle neuroscienze da molto tempo (Galaburda, et al., 1978; Rubino, 1970) e una delle funzioni cerebrali lateralizzate storicamente e maggiorment studiate è il linguaggio. Recentemente, diversi studi hanno utilizzato la tecnica di diffusion tensor imaging (DTI) per descrivere i tratti di materia bianca correlati al linguaggio nell'emisfero sinistro (Barrick, et al., 2007; Bernal & Altman, 2010; Catani, et al., 2007; Glasser & Rilling, 2008; Hagmann, et al., 2006; Parker, et al., 2005; Propper, et al., 2010; Upadhyay, et al., 2008; Vernooij, et al., 2007). Inoltre, studi su lesioni e studi fMRI in soggetti sani hanno dimostrato che la comprensione e la produzione linguistica sono funzioni che pertengono all'emisfero sinistro (A. U. Turken & Dronkers, 2011).

L'obiettivo del presente lavoro di dottorato consiste nell'approfondire la relazione tra correlati anatomici e funzionali della dominanza emisferica nel circuito linguistico persilviano. A questo scopo è stato utilizzato un approccio multimodale con DTI e fMRI applicate in una popolazione di 23 individue sani.

Nel primo studio, ho eseguito una dissezione virtuale in vivo dei tre sottocomponenti del fascicolo arcuato. In accordo con gli studi precedenti (Barrick, et al., 2007; Buchel, et al., 2004; Catani, et al., 2007; Powell, et al., 2006), ho trovato una lateralizzazione sinistra significativa nei valori di anisotropia frazionale (FA) del segmento diretto del fascicolo arcuato. Inoltre, ho trovato un'altra lateralizzazione significativa a sinistra nei valori di streamlines (SL) del segmento posteriore e una lateralizzazione significativa a destra nei valori di SL del segmento anteriore. Infine,

non è stata riscontrata alcuna evidenza di una relazione tra gli indici di lateralizzazione e le misure di performance linguistica e di memoria verbale.

Nel secondo studio, ho implementato un'analisi di connettività funzionale per testare se la lateralizzazione a sinistra negli inidici di connettività fra le regioni perisilviane prese in considerazione si osservasse mentre gli individui eseguivano un compito linguistico. Il risultato principale di questo secondo studio è stata una lateralizzazione significativa a destra nella connessione anteriore, quindi tra il giro frontale inferiore (IFG) e il lobo parietale inferiore (IPL).

Nel terzo studio, ho combinato i dati DTI e fMRI per verificare se ci fosse una relazione significati tra misure di connettività strutturale e funzionale nel circuito perisilviano e se differisse tra i due emisferi. L'analisi di correlazione ha dimostrato correlazioni negative significative tra valori medi di FA nel segmento diretto del fascicolo arcuato e la forza della connettività funzionale tra il IFG e il giro temporale medio nell'emisfero sinistro, e tra valori di FA nel segmento anteriore e la connettività funzionale tra il IFG e il IPL nell'emisfero destro. Infine, non sono emerse correlazioni significative tra gli indici di lateralizzazione calcolati sui valori di FA e di connettività funzionale.

1. INTRODUCTION

Hemispheric lateralisation in the human brain has been a focus of interest in different fields of neurosciences since a long time (Galaburda, et al., 1978; Rubino, 1970).

Studies on patient and non-patient populations have repeatedly shown that the left and right hemispheres (LHem and RHem) can be different in their structures (e.g. size, location, and/or shape of different areas) and in their information processing faculties (Cabeza & Nyberg, 2000; Gazzaniga, 2000).

One of the most studied and earliest observed lateralised brain functions is language. Reported in the nineteenth by the French physician and anatomist Paul Broca (1861) and by the German anatomist and neuropathologist Carl Wernicke (1874), language was found to be more impaired following tumours or strokes in the left hemisphere.

Broca described a postmortem examination of a patient with an area of damage in the third frontal convolution of the left hemisphere who showed a deterioration of speech production. Subsequently, Wernicke presented a postmortem examination of a patient with damage to the left posterior superior temporal cortex who had impaired speech comprehension. Wernicke hypothesised the existence of a direct connection between the two areas, and that a damage of this hypothesised pathway would cause an aphasia, characterised by normal language comprehension and fluent speech production but the incapability to repeat what had just been heard. In fact, an extended pathway connecting posterior frontal and superior temporal lobes had already been reported by the German physiologist Burdach and was later

confirmed by the French neurologist Joseph Jules Dejerine (Dejerine, 1985) who named the pathway Burdach's arcuate fasciculus. Dejerine identified the trajectories of major white matter fibre bundles, and these pathways were subsequently visualized in three dimensions (Ludwig & Klinger, 1956). The superior longitudinal or arcuate fasciculus (SLF), a long association tract connecting frontal, parietal, and temporal cortex, was seen to originate in the inferior and middle frontal gyri, projecting posteriorly before curving around the insula into the temporal lobe. Lesions causing conduction aphasias typically reside in the inferior parietal cortex and therefore cause an interruption of these fibers as they pass between Broca's and Wernicke's area. Functional hemispheric language lateralisation has proved to correlate with handedness: 95% of right-handers show functional hemispheric language lateralisation in the left hemisphere, while 15% of left-handers show functional lateralisation in the right one (Lurito & Dzemidzic, 2001; Pujol, Deus, Losilla, & Capdevila, 1999).

In recent years, a number of studies have employed diffusion tensor tractography to characterize left hemisphere language-related white matter pathways (Barrick, et al., 2007; Bernal & Altman, 2010; Catani, et al., 2007; Glasser & Rilling, 2008; Hagmann, et al., 2006; Parker, et al., 2005; Propper, et al., 2010; Upadhyay, et al., 2008; Vernooij, et al., 2007). In addition, several lesion and fMRI studies in healthy subjects have indicated that speech comprehension and production are lateralised to the left brain hemisphere (A. U. Turken & Dronkers, 2011).

In the present doctoral work I aimed to better delineate the relationship between anatomical and functional correlates of hemispheric dominance in the perisylvian language network. To this purpose I applied a multi-modal neuroimaging approach including DTI and fMRI on a population of 23 healthy individuals.

More specifically, in the first study described in Chapter 3, I carried out a virtual in vivo interactive dissection of the three subcomponents of the arcuate fasciculus and measures of perisylvian white matter integrity were derived from tract-specific dissection. In the second study, reported in Chapter 4, I implemented functional connectivity analysis to test whether leftward lateralisation of connectivity indexes between perisylvian regions can be observed in individuals performing a language-related task. Finally, in the last study described in Chapter 5, I combined DTI and fMRI data to examine whether a significant relationship is present between these measures of perisylvian connectivity and it significantly differs between hemispheres.

Important outcomes emerge from this study. First, this study confirms that white matter indexes of perisylvian language networks differ between the two hemispheres and that, in addition, the pattern of lateralisation is heterogeneous in the normal population. Secondly, unlike anatomical measures, functional connectivity indeces did not show evidence of an alike leftward asymmetry. Finally, the unexpected negative correlation observed between anatomical and functional connectivity measures in the left direct segment may reflect the complex nature of their relationship and depend specifically on the nature of the fMRI task employed in this study.

2. METHODS AND MATERIALS

2.1 Study sample

Healthy participants, ages 18 to 35, were recruited over the same period (i.e. about 15 months) and from the same socio-demographic area through local advertisement. Healthy participants had no history of psychiatric disorder and had no first degree relatives with a diagnosis of a psychotic illness.

2.1.1 Inclusion and exclusion criteria

Participants met the following criteria:

- Aged 18 to 35 years old
- Estimated premorbid IQ greater than 70
- English as a first language
- No history of severe head injury or neurological disorder
- No evidence of substance abuse and dependence disorder according to the DSM-V criteria
- No relevant visual or hearing impairment
- Contraindication to exposure to a magnetic field (i.e. presence of metal implants, old generation tattoos and pregnancy)

2.1.2 Recruitment process and informed consent

Potential participants were introduced to the present study by one of the clinicians within each of the NHS teams mentioned above. An information sheet with a detailed outline of the purposes and procedures of the study was given to those clients showing interest in participating in the research project. Whenever possible, a face-to-face meeting was arranged where the study was discussed in further detailed and inclusion/exclusion criteria were verified. Alternatively, a telephonic screening interview was carried out. All participants were invited to give written informed consent and they were informed that they could withdraw from the study at any time without providing any explanation.

2.1.3 Sample Size

While the process of power and sample size analysis is relatively straightforward in behavioural studies, in neuroimaging studies power calculation is a more problematic process. The neuroimaging community has extensively discussed the argumentations for and against the application of standard single-outcome power analysis to neuroimaging data (Desmond & Glover, 2002; K. J. Friston, Holmes, & Worsley, 1999; Mumford & Nichols, 2008). First, in neuroimaging studies the outcomes refer to 3D images in which the signal in tens of thousands of voxels is spatially and, in the case of fMRI studies, temporally correlated. This means, in turn, that the statistical power depends not only on the effect size itself but also on the extent of the effect, i.e. the number of voxels for which the null hypothesis is false. Second, both the size and the variability of the effect are required in order to estimate statistical power for a given sample size. The specification of variance is

particularly difficult for group comparisons based on neuroimaging data where the variance is determined by a combination of within-subject (first level analysis) and between-subject (second level analysis) variance. Moreover, the variance parameters are not often reported in neuroimaging studies and the estimated covariance structures themselves differ across the different software packages available. Most importantly, if the size and the variability of the effect were already available with precision, there would be no need for the study to be performed in the first instance. There have been few attempts to develop procedures to estimate statistical power in fMRI studies, such as efficient first level study design specifications, simulations and resampling-based methods; however none of them has resulted in a well-established procedure (Desmond & Glover, 2002; Mumford & Nichols, 2008).

A total of 23 healthy participants were recruited. For some subjects, however, imaging data from one or more modalities were not included in the statistical analysis due to technical difficulties encountered during the collection of imaging data (i.e. acquisition artefacts and excessive head movements). Therefore, the number of participants varies slightly for different imaging modalities and is reported, accordingly, in each experimental chapter of this thesis.

2.1.4 Pre-scan clinical interview and neuropsychological assessment

All participants were interviewed prior to scanning by the candidate and a colleague. The interview covered family and personal psychiatric history, current and past medication treatment as well as current and past history of alcohol and drug use. The presence and severity of depression, anxiety and stress symptoms

were further characterised by using The Depression Anxiety Stress Scale (Crawford & Henry, 2003). The Lateral Preference Inventory (Coren, 1993b) was employed to assess participants handedness. The reading subtest from the Wide Range Achievement Test-Revised (Reynolds, 1984) was used to evaluate the premorbid verbal intelligence. The WRAT-R has proved to be an adequate predictor of Wechsler Adult Intelligence Scale-Revised (WAIS-R) IQ scores and, when compared to the North American Adult Reading Test (NAART), the WRAT is thought to yield a more accurate estimate for lower VIQ ranges (Johnstone, Callahan, Kapila, & Bouman, 1996). Finally, the 'FAS' letter sequence and animal naming subtests from the Controlled Word Association Test were administered to assess phonemic and semantic verbal fluency (Loonstra, Tarlow, & Sellers, 2001).

2.2 Acquisition of Magnetic Resonance Imaging data

Structural MRI (sMRI), functional MRI (fMRI) and diffusion tensor imaging (DTI) are analytical techniques that make use of the property of nuclear magnetic resonance (NMR) to image nuclei of atoms and their properties in the body. NMR represents the capability of magnetic nuclei in a magnetic field to absorb and re-emit electromagnetic radiation. This phenomenon occurs at a specific resonance frequency, which depends on the strength of the magnetic field as well as the magnetic properties of the specific isotope of the atoms. Since the resonance frequency is directly proportional to the strength of the applied magnetic field, if a sample is placed in a non-uniform magnetic field then the resonance frequencies of the sample's nuclei will depend on their location within the magnetic field: this

property represents the key NMR feature that neuroimaging techniques exploit in order to image brain nuclei of atoms and their properties.

2.2.1 Structural MRI

Protons composing any atomic nucleus have the intrinsic quantum property of spin by which they revolve around an axis and produce a magnetic field with a north-south polarity along the spin axis (i.e. the magnetic vector). In the presence of an intrinsic and static magnetic field, individual spins are randomly orientated and bulk material has no magnetisation. If a nucleus is exposed to an external magnetic field B_0, however, the individual magnetic spins will start precessing around the direction of the applied magnetic field. In the human body most of the atomic protons are found in the hydrogen atoms contained in water. The hydrogen nucleus spins can present with two orientations relative to the applied magnetic field B_0: (i) the parallel orientation associated with a low-energy state and (ii) the anti-parallel orientation associated with a high-energy state. Therefore, the net magnetisation of the object placed in the applied magnetic field derives from the sum over all the hydrogen nuclei in the object. Its representation is based on an orthogonal *zxy* coordinate system with the *z-axis* encoding the direction of the applied magnetic field B_0. Since in a resting magnetisation state more spins are in the low- rather than in the high-energy state, the sum of each singular magnetic vector will result in a net magnetic vector M_0.

When an oscillating radiofrequency electromagnetic field B_1 is applied that is perpendicular to the main magnetic field B_0, the individual spins can be excited and shift from a low- to high-energy state. This phenomenon occurs most efficiently in

the presence of resonance frequency, thus when the oscillating frequency of the B_1 and the frequency of the protonic spins are equal. As a consequence of applying a radiofrequency pulse B_1, the protons are brought into coherence and the individual magnetic vectors shift to point all in the same direction of the applied magnetic field resulting in a new magnetic vector M_1 on the *xy* transverse plane. The transversal component of the new magnetic vector M_1 induces an electrical current that is detected by a coil on the *xy* plane and determines the formation of an NMR signal. However, using a homogenous magnetic field would not yield a tomographic image since all protons within the sample will be exposed to the same magnetic field and, therefore, the frequency of their emitted signal would be identical. Instead, a non-uniform magnetic field is applied that allows variations of resonance frequencies of spin within the sample.

After excitation, the spin system will release the absorbed energy and gradually return to the initial equilibrium state. This relaxation occurs through two processes:

1. *Spin-lattice or T1 relaxation.* Energy is transferred to neighbouring molecules in the surrounding structure. T1 relaxation relates to the recovery of the M_0 along the *z* axis and its exponential temporal function is described by the T1 time constant. Since the nuclei energy is dissipated to molecules of the surrounding structure, heat and composition of the environment will affect T1.

2. *Spin-Spin or T2 relaxation.* Energy is transferred to the nearby nuclei. T2 relaxation relates to the disappearance of coherence in the transversal magnetic field M_1, which occurs at a different rate to the recovery of magnetisation along the *z* axis. No energy is lost in this process but the transfer of energy between protons results in a gradual decrease of M_1.

The use of different B_1 magnetic gradients will induce protons to emit different frequency signals depending on their spatial position within the sample. It follows that the known value of the applied strength and direction of the magnetic field can be used to determine the position from which the signal was emitted. Nevertheless, acquiring only frequency measures of the signal would result in its spectrum to be a one-dimensional representation of spin density in each slice. Therefore, to produce a two-dimensional image requires encoding information on a second axis. For this purpose, location-dependent phase is obtained by using a further gradient (spin echo), which is a pulse used to dampen the loss of transversal magnetisation. As a result, locations are encoded by frequency on the first axis and phase on the second axis. Subsequently, the sample is subdivided into volume-elements or voxels by using step-wise increases in both gradients and the step size of the gradients determines the size of the voxels. Therefore, the final image of multiple frequencies provides spatial information, derived from its orthogonal gradients magnetic fields, and contrast information, obtained from its relaxation parameters that can be visualised and further analysed depending on the specific MRI modality of interest.

2.2.2 Diffusion Tensor Imaging

DTI is a MRI technique that exploits the property, known as random walks (Brown, 1828), of water molecules undergoing diffusion in living tissue to obtain information about brain white matter integrity and connections. More specifically, each water molecule stays in a particular place for a fixed time T before to move, randomly, to a new location within the space. Although it is not possible to accurately predict the pathway that each molecule can take, it is known that the squared displacement of

molecules from their starting point over a time *t* is directly proportional to the observation time (Einstein, 1905). Therefore, the squared displacement can be predicted by using the self-diffusion coefficient specific to water molecules undergoing diffusion at body temperature. In diffusion MRI, the mean displacement of water molecules is measured within each voxel in the brain where the presence of cell membranes and macromolecules hinder their random walk pathway. As a consequence, the mean displacement from a starting point in a fixed period of observation is reduced compared to their mean displacement in 'free' water and is referred to as apparent diffusion coefficient (ADC). The average ADC in tissue is about 4 time smaller than in free water.

In order to sensitise the MR signal to diffusion, a diffusion weighted (DW) sequence is required that impose a specific phase to a molecule that is dependent on its main displacement (Stejskal & Tanner, 1965). Under the diffusion process, several displacements are encoded and this leads to a spread distribution of related phases. The diffusion process yields a distribution of different displacements and, therefore, to a spread of displacement-dependent phases. In turn, this spread of phases results in a loss of signal coherence and a reduction in signal amplitude (i.e. dark areas are observed in the MR image). In other words, the greater the diffusion, the greater the loss of signal and the darker the final image. The DW sequence employed in the present study is reported in details in chapter 3, section 3.2.4

In the human brain white matter the diffusion coefficient appears to be directionally dependent, that is it depends on the direction of the applied diffusion-encoding gradient (Chenevert, Brunberg, & Pipe, 1990; Doran et al., 1990). The diffusion tensor is a complex model that characterises Gaussian diffusion in which the displacements per unit time are not the same in all directions. It corresponds to a 3

by 3 symmetric matrix of numbers in which the diagonal elements represent diffusivities along the three orthogonal axes (Jones, 2008). The tensor is derived by collecting several samples of the DW signal and is estimated from these signals using a multivariate regression (Beaulieu & Allen, 1994). Diffusion is described as isotropic when the DW intensity is the same for each diffusion-encoding gradient applied along the three orthogonal axes in a brain region, while is referred to as anisotropic when the DW intensity varies across the three axes diffusion (Jones, 2008). Thus, if there is strong attenuation of diffusion signal for a specific direction (e.g. left-right orientation) one can infer that diffusion is relatively unhindered along this direction. Conversely, if the signal attenuation is minimal, and so the mean displacement, one can infer that something is hindering the diffusion of water molecules along these orthogonal axes. By using the direction-specific information is therefore possible to infer the presence of an ordered structure which as a predominant orientation. To date, the most commonly used anisotropy index is fractional anisotropy (FA) that measures the fraction of tensor that can be assigned to anisotropic diffusion. FA measures are appropriately normalised and take values from 0, when diffusion is isotropic, to 1 when diffusion is constrained along one axis only (Basser & Pierpaoli, 1996).

2.2.3 Functional MRI

fMRI is a non-invasive analytical technique that can be used to infer neural activity, related to mental operations during the performance of a specific task, by assessing changes in local blood oxygenation. Regional increases in neuronal activity are associated with increases in blood flow that sustain changes in local oxygen

consumption. More specifically, the net oxygenation (i.e. the ratio of oxygenated to deoxygenated haemoglobin) of the blood in a neuronally activated brain region is increased (Ogawa et al., 1993). The blood oxygen level-dependent (BOLD) contrast (Ogawa, Lee, Kay, & Tank, 1990) reflects metabolic activity in the brain tissues and relates to the magnetic susceptibility of brain tissue, oxyhaemoglobin and deoxyhaemoglobin (Pauling & Coryell, 1936). While oxyhaemoglobin is weakly diamagnetic and, therefore, has a trivial effect on the surrounding magnetic field, deoxygenated haemoglobin features paramagnetic properties and is able to introduce a lack of homogeneity into the neighbouring magnetic field. Therefore, an increase in deoxyhaemoglobin concentrations acts as an endogenous paramagnetic MRI contrast yielding a reduction of image intensity. The function that describes the theoretical relationship between neuronal firing and BOLD signal is referred to as the haemodynamic response, which can be characterised by three sequential phases (Buxton, Wong, & Frank, 1998; Vanzetta & Grinvald, 2001). First, a moderate reduction of image intensity occurs that is due to an initial period of oxygen consumption. Subsequently, the signal presents a large intensity increase due to regional excess of oxygenated blood. Finally, a reduction of signal intensity is associated with a decreasing supply of oxygenated blood, which leads to the initial equilibrium state. Therefore the BOLD signal reflects a complex interaction between cerebral blood flow, cerebral blood volume and oxygenation. Physiologically validated models suggest that the mechanism initiating vasodilatatory and oxygenation changes may be driven by neuronal-glial interactions following a neurotrasmitter release (Buxton, et al., 1998; Magistretti & Pellerin, 1999). Moreover, microelectrode studies in animals report that changes in BOLD signal is associated with pre-synaptic activity and reflects input and intra-cortical processing

in the mapped brain area as opposed to output and post-synaptic transmission (Goense & Logothetis, 2008; Viswanathan & Freeman, 2007). This evidence seems to support the notion that the inferred neuronal activity is driven primarily by synaptic, rather than spiking, activity. fMRI can provide accurate localisation of neuronal activity since changes in arteriolar blood flow are spatially matched to the sites of increased neuronal activity (Logothetis & Pfeuffer, 2004). Compared to sMRI acquisition, collection of fMRI data requires a different pulse sequence that is sensitive to functionally determined changes in signal intensity. The most frequently used acquisition sequence is a combination of gradient echo sequences and echo-planar imaging (EPI). This combination allows very rapid data acquisition and provides multislice images of the whole brain with a slice thickness of a few millimetres. The fMRI acquisition sequence used in the present study is reported in details in chapter 4, section 4.3.2.

2.2.3.1 fMRI experimental design

In fMRI a functionally specific neurovascular response is obtained by manipulating the subject's experience or behaviour through the application of an appropriate experimental design. At present, two classes of experimental design are commonly used: block and event-related.

Blocked Design. When this design is applied, participants are asked to perform a mental task of interest alternated with one or more other tasks of no interest; in the simplest form, the activation (A) condition of interest is alternated with a baseline (B) condition. Each condition represents an epoch during which several stimuli are presented sequentially to the participant with an inter-stimulus interval (ISI) that

varies depending on the specific experimental paradigm. The alternation between activation and baseline condition can be repeated several times over the experiment length. The different task conditions are usually matched in all respects with the exclusion of those specifically related to the cognitive process of interest. The basic assumption in block experimental design is known as cognitive subtraction (K. J. Friston, Holmes, Poline, Price, & Frith, 1996). According to this assumption, only those brain areas that are specifically involved in a certain cognitive process will show increased MRI signal intensity during that condition. In contrast, brain regions responsible for aspects of the task that are also present in the baseline condition, such as visual and motor processes, will be activated identically across the two conditions and will not present with a periodic signal change as the two conditions are alternated. Therefore, block designs can be applied with the aim of detecting the steady state brain activation during each task condition as well as identifying where in the brain a specific task condition induces different levels of activation. Block experimental designs have the advantage of generating robust signal changes but do not allow the investigation of response to a specific stimulus. This experimental design was employed in the present study; information about the specific experimental paradigm and design can be found in chapter 4, section 4.3.1.

Event-related design. In this type of experimental design, individual trials related to different task conditions are presented sequentially, in a random order and with longer ISIs compare to those used in block designs. Since they allow investigation of response to a specific stimulus, event-related designs can be employed whit the aim to measure the brain activity that is time-locked to each individual trial and, as for the block design, to detect where in the brain different trial types exert different level of activation (Dale, 1999; Zarahn, Aguirre, & D'Esposito, 1997). In addition, this

type of experimental design is better suited to experimental conditions where specific trial types are assigned post-hoc on the basis of the subject's previous responses. However, event-related designs have the disadvantage of generating intensity signal changes that are weaker compared to those generated by block designs.

2.3 Analysis of MRI data

2.3.1 Univariate analysis of structural and functional MRI data

A number of packages are available for the analysis of structural and functional imaging data. Statistical parametric mapping (SPM) is, amongst all, the most common analytical approach and was employed in this thesis as implemented in SPM8 software (http://www.fil.ion.ucl.ac.uk/spm), running under MATLAB 7.4 (MatWorks, Natick, MA, USA). This approach entails the definition of spatially extended statistical processes to test hypotheses about regionally structural or functional specific effects (K. J. Friston et al., 1995); these processes are referred to as statistical parametric maps (SPMs). SPMs are voxel-based image processes in which voxel values are, under the null hypothesis, distributed according to a known probability density function, typically the Student's t or F distributions. Thus each voxel in the brain is first analysed using a standard univariate statistical test and these statistical parameters are then assembled into the SPM image. The probabilistic behaviour of Gaussian fields (Worsley et al., 1996) is used to interpret SPMs as spatially extended statistical processes and Gaussian random fields (GRF) model both the univariate probabilistic characteristics of a SPM as well as any non-stationary covariance structure.

Pre-processing. Prior to statistical analysis original images need to be pre-processed in order to make imaging data suitable for parametric approaches and therefore ensure the validity of subsequent parametric statistical tests. Pre-processing procedures varies between analysis of structural and functional imaging data; for the present study, detailed descriptions of the pre-processing procedures applied to structural and functional MRI data are described in chapter 3 (section 3.2.4) and chapter 4 (section 4.3.4) respectively.

Statistical Analysis. Following the initial pre-processing, differences in regional grey matter volume (in sMRI) and BOLD signal (in fMRI) are estimated in a voxel-specific fashion using a variant of the General Linear Model (GLM). The GLM attempts to explain the sMRI or the fMRI signal in terms of the weighted sum of a number of variables of interest corresponding to the hypothesised effects. A set of regressors is used to encode the variables of interest and multiple linear regression is used to estimate the parameter estimates for these regressors at each voxel, together with an error term that reflects variability in the observed time series that cannot be accounted for by the hypothesised effects. After model estimation, standard parametric statistics (t-test and F-test) are applied to the size of the parameter estimates relative to the error term in order to test hypotheses about differences between effects of interest and the results are reported in SPMs. Therefore, an SPM represents a large distributed collection of t or F values that is typically displayed as a three-dimensional rendering onto cortical surface anatomy or as a two-dimensional overlay onto individual slices of a T1-weighted anatomical image.

Since at this stage many voxel-wise tests are computed, as each image volumes can contain over 100,000 separate observations (voxels), a statistical threshold must be chosen that determines the lower bound of statistical values to display in the SPM.

The definition of a significance threshold represents a particular issue for neuroimaging data. In fact, it is likely that grey matter as well as regional activation in neighbouring voxels will be highly correlated and thus a correction for multiple comparisons with a classical Bonferroni approach will be inappropriate. The Gaussian GRF theory is used to solve this multiple comparison problem and to derive an alternative approach to standard Bonferroni correction. A random field is a list of random numbers whose values are mapped onto a space of *n* dimensions and spatially correlated so that adjacent values do not differ as much as values that are further apart. This theoretical framework, thus, provides a more appropriate method for correcting *p* values for the search volume of a SPM (K. J. Friston, et al., 1996; Worsley, et al., 1996). The risk of error that one is prepared to accept is called the Family-Wise Error (FWE) rate and represents the likelihood that a family of voxels values, as opposed to a single voxel value, could have arisen by chance. A threshold of $p<0.05$, FWE corrected, is conventionally used.

2.3.2 Diffusion Tensor Imaging analysis

In ordered tissue structures, robust and readily interpreted fibre orientation can be derived by using the information within the diffusion tensor and, more specifically, from the principal eigenvector associated with the largest eigenvalue (Pierpaoli, Jezzard, Basser, Barnett, & Di Chiro, 1996). The components of the orientation of the fibre are then represented using different primary colours to create a colour encoded fibre orientation map. According to the direction scheme proposed by Pajevi and Pierpaoli (1999), fibres that are predominantly oriented left-right are shown in red, anterior-posterior fibres are shown in green and superior-inferior

fibres are shown in blue. It follows that colour fibre orientation maps provide more information than anisotropy maps alone.

2.3.2.1 White matter bundles tractography

The purpose of fibre tracking is to derive the three-dimensional trajectories of anisotropic structures in tissue by assembling together discrete voxel-based estimates of the underlying continuous orientation field (Basser, Pajevic, Pierpaoli, Duda, & Aldroubi, 2000; Mori & van Zijl, 2002). Tractography approaches are usually classified into two types: deterministic and probabilistic.

Deterministic tractography. The basic assumption in deterministic tractography is that the principal eigenvector is parallel to the underlying dominant fibre orientation in each voxel and tangent to the space curve described by the white matter tract (Basser et al. 2000). Therefore, it is possible to infer the evolution of the space curve by propagating a single pathway bi-directionally from a 'seedpoint' and moving in a direction that is parallel with the principal eigenvector. Since it is assumed that the underlying tensor field is continuous, sub-voxels estimates of the tensor are required in this approach and obtained either by interpolation of the raw DW images or by interpolation of the tensor elements (Conturo et al., 1999; Mori & Barker, 1999). In deterministic tractography, two arbitrary thresholds are usually employed to constrain tract dissections. First, in order to differentiate white matter from grey matter, tracking is terminated if the front of the tract enters a site where the anisotropy is below a fixed value. Second, an angular threshold is applied that specifies the maximum angle that the path can describe between one step and the next, which prevent reconstruction of 'unfeasible' pathway turns. To date, however,

there is no general consensus as to the value of this angular threshold (Jones, 2008). When using deterministic tracking packages, the user selects more than one seedpoint from which to start tracking and also a region of interest (ROI) that, based on anatomical knowledge, intersects the fasciculus of interest. It follows that a successful tract reconstruction is dependent on the skill and neuroanatomical knowledge of the user. Nevertheless, deterministic tractography has proven to produce anatomically faithful reconstructions of white matter bundles (Catani, Howard, Pajevic, & Jones, 2002; Mori & van Zijl, 2002)

Probabilistic tractography. In this approach, a large number of pathways are propagated from a selected seedpoint, as opposed to a single trajectory as is performed in deterministic approaches. At each stage of the process that delineate the path, the direction in which to step next is drawn from a distribution of possible orientations. This process results in a set of multiple pathways passing through the seedpoint and a percentage of pathways, launched from the seedpoint, that pass through each voxel in the set. Since, unlike deterministic approaches, probabilistic tracking algorithm do not depend on the principal eigenvector, they typically do not employed an anisotropy threshold for termination of tracking (Behrens, Rohr, & Stiehl, 2003; Parker, Haroon, & Wheeler-Kingshott, 2003) Different probabilistic approaches can be used that differ between each other in the mechanism by which the inherent distribution of fibre orientations is drawn (Jones, 2008). Nevertheless, they all result in a map that attempts to quantify, for each seedpoint, how confident one can be that a pathway can be found between each voxel and that specific seedpoint. These maps represent the likelihood of a connection through the data given the samples of the data and are, therefore, strongly dependent on the quality of the data.

In the present study, a deterministic approach was used to perform a virtual in *vivo* interactive dissection (Catani, et al., 2002) of the main white matter bundles of interest. This approach was chosen as it provides tract-specific measurements, such as fractional anisotropy, mean diffusivity and volume, allowing the quantification of microstructural integrity of specific white matter tracts and their subcomponents. The pre-processing and tractography procedures are described in details in chapter 3, 3.2.4 and 3.2.5 respectively.

2.4 Inter-regional interactions

In addition to regional task-dependent activity, the analysis of fMRI data can also provide information about inter-regional interactions (functional integration) and how they vary according to behavioural or physiological states (Buchel & Friston, 1997). When characterising and assessing functional integration in the brain, a fundamental distinction is that between functional and effective connectivity (K J Friston, 1994).

2.4.1. Functional connectivity and correlation analysis

Functional connectivity refers to a covariance between time-dependent activity in different brain areas regardless of any specific directional effects or whether an anatomical connection exists that links those areas. Thus, it solely represents a statistical dependency among measurements of spatially remote neurophysiological events. In its simplest form, functional connectivity between two regions can be

assessed by using Pearson's correlation analysis. Typically, a standard fMRI analysis is initially performed to identify regions that show task-related activity (if regions of interest, ROIs, are not selected on the basis of a clear a-priori hypothesis) and to determine the stereotactic coordinates corresponding to subject-specific local maxima within a selected region. Subsequently, subject-specific time-series are extracted from the coordinates of each ROI and Pearson's correlation analysis is applied to assess the relationship between time-series. Brain ROIs selection and extraction of time-series procedures for the functional connectivity analysis, performed as a part of the present doctoral project, are described in detailed in chapter 4, section 4.2.7.

3. INVESTIGATING LATERALISATION IN THE LANGUAGE NETWORK: A DTI STUDY

3.1 Introduction

In recent years, a number of studies have employed diffusion tensor tractography to characterize left hemisphere language-related white matter pathways (Barrick, et al., 2007; Bernal & Altman, 2010; Catani, et al., 2007; Glasser & Rilling, 2008; Hagmann, et al., 2006; Parker, et al., 2005; Propper, et al., 2010; Upadhyay, et al., 2008; Vernooij, et al., 2007). This technique, known as diffusion tensor tractography, is a non-invasive method for examination of white matter architecture and therefore, the underlying connectivity of the brain.

Buchel et al. (2004) were among the first to investigate white matter asymmetry in the human brain through the means of diffusion tensor MRI. They examined 2 independent groups of subjects with DTI. The first sample comprised 15 right-handed healthy subjects, while the second comprised 28 healthy subjects, including 21 who were right-handed and 9 who were left-handed. The results, obtained by using voxel-based statistics on fractional anisotropy (FA) maps derived from DTI, showed a leftward asymmetry in the arcuate fasciculus and an additional effect of handedness, with a significant larger FA in the precentral gyrus controlateral to the dominant hand.

Also (Nucifora, Verma, Melhem, Gur, & Gur, 2005) reported a robust leftward asymmetry in the relative fibre density (the ratio of the number of the arcuate tracts

to the total number of fibre tracts genterated in the arcuate ROI) of the arcuate fasciculus of 27 right-handed healthy volunteers who were assessed with DT-MRI.

Another study employed diffusion-weighted MRI to examine the auditory-language pathways in the human brain of 11 right-handed subjects (Parker, et al., 2005). Based on the results of studies on primates that showed a ventral pathway - projecting anteriorly from the primary auditory cortex to prefrontal areas along the superior temporal gyrus – and a dorsal route - connecting these areas posteriorly via the inferior parietal lobe (Kaas & Hackett, 1999; Romanski et al., 1999), the authors examined the possibility of a similar pattern of connectivity in the human brain. The results showed a connection between Wernicke's and Broca's area via arcuate fasciculus in both hemispheres, and a second ventral pathway between these auditory-language centres, the existence of which has been proposed as a result of nonhuman primate studies (Hickok & Poeppel, 2000; Rauschecker, 1998). The volume occupied by the identified connective pathways in the left hemisphere was greater than in the right, implying larger anatomical connectivity. The ventral pathway was exclusively found in the left hemisphere, which is in keeping with functional neuroimaging results reporting only left hemisphere activation for processing intelligible speech (Romanski, et al., 1999; Scott, Blank, Rosen, & Wise, 2000).

Another DT-MRI tractography study (Hagmann, et al., 2006) showed that right-handed men are more lateralised than women. The axonal connectivity between Wernicke's and Broca's areas and their right hemisphere homologues was investigated in 32 subjects (16 men, 8 RH and 8 LH; and 16 women, 8 LH and 8 RH). Each ROI was selected on functional activation maps from the study population. Stronger connections between Wernicke's and Broca's areas compared to their

homologues in the right hemisphere were found in men. Also the study evidenced that women and left-handed men have equally strong intrahemispheric connections in both hemispheres, but women have a higher density of interhemispheric connections.

The leftward asymmetry of white matter organisation associated with language function was also found by (Barrick, et al., 2007) through the means of diffusion weighted-MRI applied to 30 right-handed healty volunteers (15 males). Specifically, the results showed a significant leftward lateralisation of the pathway connecting the posterior temporal lobe through the posterior segment of the arcuate fasciculus to the supramarginal and angular gyri. Also, 2 significant leftwardly asymmetric temporofrontal pathways were evidenced connecting the posterior temporal lobe to the frontal lobes. The first passed along the long segment of the arcuate fasciculus to the precentral gyrus and pars opercularis, whereas the second was a medial pathway through the external capsule to the pars triangularis and pars opercularis.

In another study (Glasser & Rilling, 2008) DTI deterministic tractography was employed to define the hypothesised leftward asymmetry in the arcuate fasciculus with respect to both anatomy and function, and also combine our findings with a recent model of brain language processing to explain 6 aphasia syndromes. The arcuate fasciculus of 20 right-handed males was divided into 2 segments with different hypothesized functions, one terminating in the posterior superior temporal gyrus (STG) which computes phonologic processing and another, terminating in the middle temporal gyrus (MTG), which treats lexical and semantic information. Tractography results were evaluated in comparison with peak activation coordinates from prior functional neuroimaging studies of phonology, lexical-semantic and prosodic processing to give accepted functions to these pathways. STG

terminations were strongly left lateralised and overlapped with phonological activations in the left but not the right hemisphere, advocating for the hypothesis that exclusively the left hemisphere phonological cortex is directly connected with the frontal cortex via the arcuate fasciculus. A leftward asymmetry was found also for MTG terminations, overlapping with left lateralised lexical-semantic activations. Smaller right hemisphere MTG terminations overlapped with right lateralised prosodic activations.

In contrast with all the previous studies, the results obtained by (Bernal & Altman, 2010) showed that the main anterior endpoint of the superior longitudinal fasciculus was situated in the precentral gyrus (premotor/motor area) and not in the Broca's area of the left hemisphere. The investigation focused on the connectivity of the superior longitudinal fasciculus using DTI tractography on 12 right-handed healthy volunteers, aiming to determine whether the arcuate fasciculus, or any of the fibres in the superior longitudinal fasciculus, terminates in the Broca's area. This finding would explain the lack of correlation between lateralisation of the superior longitudinal fasciculus and language areas reported by some studies.

In the present we study aimed to examine the cerebral lateralisation of the arcuate fasciculus organisation imaged by mapping water diffusion characteristics from diffusion-weighted MRI. In particular, I investigated language-related asymmetry in the left hemisphere reported in the previous studies using the model of language network proposed by (Catani, Jones, & ffytche, 2005), which is the main aspect of novelty of this study. The model includes a direct phonetic pathway (via the arcuate), between Wernicke's and Broca's areas acting in automatic, fast word

repetition, and an indirect semantic pathway (via 2 segments that connected the inferior parietal lobe to both the temporal and frontal lobes), where a stage of verbal comprehension and semantic/phonological transcoding intervenes between verbal input and articulatory output. The existence of two pathways with such functions is supported by evidence from patients with aphasic syndromes (Boatman et al., 2000; Damasio & Geschwind, 1984; Schiff, Alexander, Naeser, & Galaburda, 1983).

We aimed to explore also the possible lateralisation and involvement of other tracts in language, such as the cingulate bundle and the uncinate fasciculus for which there is already some evidence that it might play a role, even though not crucial (Duffau, Gatignol, Moritz-Gasser, & Mandonnet, 2009; Galantucci et al., 2011; Papagno, 2011). In addition we correlated the lateralisation index of the reconstructed arcuate fasciculus and the performances in the California Verbal Learning Test (CVLT; total words recall) since significant positive correlation was found by (Catani, et al., 2007).

The following hypotheses were tested:

1) A leftward hemispheric asymmetry would be found in the arcuate fasciculus, predominantly in the long direct segment connecting frontal and temporal regions.

2) A positive correlation would be found between the lateralisation index of the arcuate fasciculus and the performances in the CVLT.

3) For completeness and for comparison, we also investigated the lateralisation distribution of other to white matter tracts - the cingulate bundle and the uncinate fasciculus – for which there is evidence that they might play a role, although not crucial, in the language network.

3.2 Methods

3.2.1 Participants

Participants were 23 healthy individuals without any current or previous evidence of psychiatric disorders recruited through advertisement from the local South London community (see chapter 2, section 2.1 to 2.1.4, for a detailed description of the demographic characteristics of the subjects and the inclusion/exclusion criteria)

3.2.2 Language skills measures

The participants were assessed were assessed with a battery of neuropsychological tests tapping language and verbal memory skills. Phonetic and semantic fluency was tested by using the FAS and animal-fruit naming tests (Delis-Kaplan, executive function). Word repetition from the aphasia battery was used to measure word repetition skills. The California Verbal Learning Test-II (CVLT-II; Delis et al., 1988; Pearson Assessment) was administered to assess individual's verbal learning and memory abilities. Along with recognition and recall scores, measures of encoding strategies, learning rates and error types were obtained. The CVLT includes five learning trials of a 16-word list. The list is read aloud by the examiner, and the examinee is instructed to freely recall as many words as possible, in any order. Each of the 16 words belongs to one of four categories of ''shopping list'' items (i.e., fruits, herbs and spices, articles of clothing and of tools). The idea underlying the CVLT is that lists of words are easier to remember if they are broken down by using a strategy of grouping them into semantic categories. After the first trial, the same 16-word list is reread aloud by the examiner, and the examinee is asked to recall again as many words as possible. The same procedure is used for the remaining three

trials. The CVLT assesses encoding and retrieval of a list of auditorily presented words. Because each word in the list can be categorized in one of the four "shopping list" groups and can therefore be clustered together with other semantically associated words, the CVLT is considered a test that does not examine verbal memory in itself, but rather some level of interaction between verbal memory and conceptual ability (Lezak, Howieson, & Loring, 2004).

3.2.3 Image Acquisition

Imaging data were acquired on a 3.0 tesla GE Signa Exite system (Milwaukee) at the Centre for Neuroimaging Sciences. The imaging protocol is summarised in the following table:

Image sequence	DTI
Slice locations	60
Images for location	--
Slice Thickness/Gap	2.4/0.2
TE	104.5
TR	14.364
Matrix	128x128

3.2.4 DTI data processing and statistical analysis

The analysis of DTI data was carried out in collaboration with the NATBRAINLAB group (http://www.natbrainlab.com/). . The diffusion tensor in each voxel was estimated using non-linear regression and a continuous description of the tensor

field was obtained using the B-spline basis field approach (Jones & Basser, 2004; Pajevic, Aldroubi, & Basser, 2002). A tracking process, using a 4th-order Runge-Kutta streamline propagation method (Basser, et al., 2000), was initiated from our regions of interest (ROIs). Additional Boolean logic operations (i.e. AND, NOT) was used to obtain a clean 'virtual dissection' (Catani, et al., 2005) of the arcuate fasciculus (long segment connecting Broca's and Wernickes' regions; indirect posterior segment connecting Wernicke's and Geschwind's territories and indirect anterior segment connecting Geschwind's and Broca's territories), the corpus callosum, the cingulum and the uncinate fasciculus. Once the tracts were dissected, measurements of number streamlines (tract volume), fractional anisotropy (FA) and mean diffusivity were obtained for each stramline and an average computed for each segment. A repeated measurement analysis was performed with hemisphere, segment, and group as factors.

3.2.5 Dissection of white matter tracts

The virtual dissection of white matter tracts of interest has been done in this study according to the diffusion tensor imaging tractography atlas for virtual in vivo dissections (Catani & Thiebaut de Schotten, 2008). This approach, which consists in defining the ROIs manually, may overcome some of the problems raised by the alternative strategy of the automatic application of normalised cortical or subcortical masks to single brain data sets, for example its proneness to generate artefactual reconstructions of tracts as a result of high uncertainty of the fibre orientation in the cortical voxels or surrounding white matter (Jones, 2003, 2008). On the other hand, the method of defining the ROIs manually embodies a different

limitation, that is it requires a priori knowledge of the white matter pathways anatomy to identify their course and delineate ROIs on DTI images.

(Catani & Thiebaut de Schotten, 2008) created a 3D tractography atlas of the associative, commissural and projection tracts in a Montreal Neurological Institute standardized system of coordinates (MNI space). In the present work the atlas was used as anatomical reference in the virtual dissecting of the following white matter pathways, as they are reported in the atlas (Catani & Thiebaut de Schotten, 2008).

3.2.5.1 Arcuate fasciculus (see Figure 1).

Identification on the color maps: The fronto-parietal portion of the arcuate fasciculus encompasses a group of fibres with antero-posterior direction (green) running lateral to the projection fibres of the corona radiata (blue) (MNI 39 to 33). At the temporo-parietal junction the arcuate fibers arch around the lateral fissure and continue downwards into the stem of the temporal lobe (blue, MNI 31). The most lateral component of the arcuate fasciculus can be easily identified as red fibres approaching the perisylvian cortex (MNI 39 to 31).

Delineation of the ROI on the FA maps (Fig. 11): A single ROI (A) on approximately five slices (MNI 39 to 31) is used for the dissection of the arcuate fasciculus. A large half moon shaped region is defined on the most dorsal part of the arcuate (MNI 39), usually one or two slices above the body of the corpus callosum. The lowest region is defined around the posterior temporal stem (MNI 31). The medial border of the region is easy to identify in the FA maps as a black line between the arcuate and the corona radiate (MNI 39 to 33) (this line should not be included in the ROI).

The lateral border of the ROI passes through the bottom part of the frontal, parietal and temporal sulci. The precentral sulcus demarcates the anterior border of the ROI (MNI 39 to 33), the intraparietal sulcus its posterior border (MNI 39 to 35).

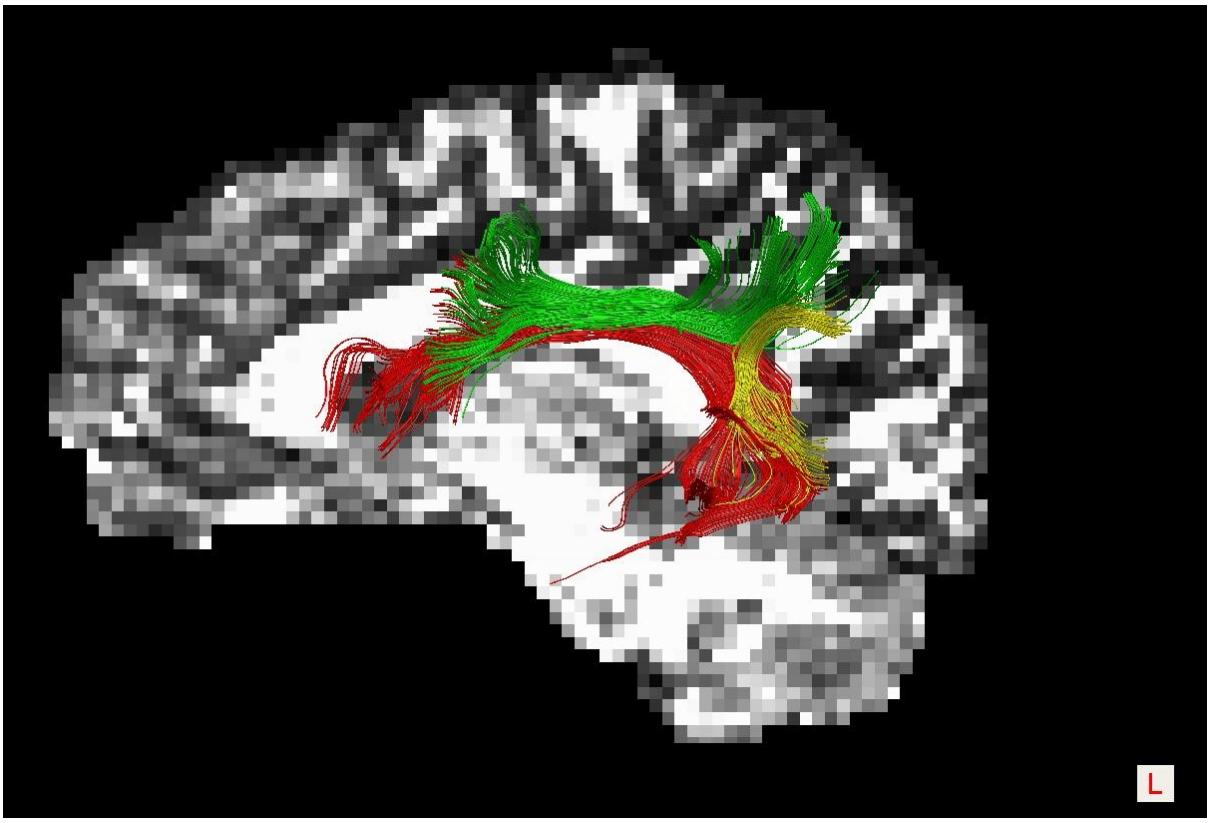

Figure 3.1. The direct pathway (long segment shown in red) runs medially and corresponds to classical descriptions of the arcuate fasciculus. The indirect pathway runs laterally and is composed of an anterior segment (green) connecting the inferior parietal cortex (Geschwind's territory) and Broca's territory and a posterior segment (yellow) connecting Geschwind's and Wernicke's territories.

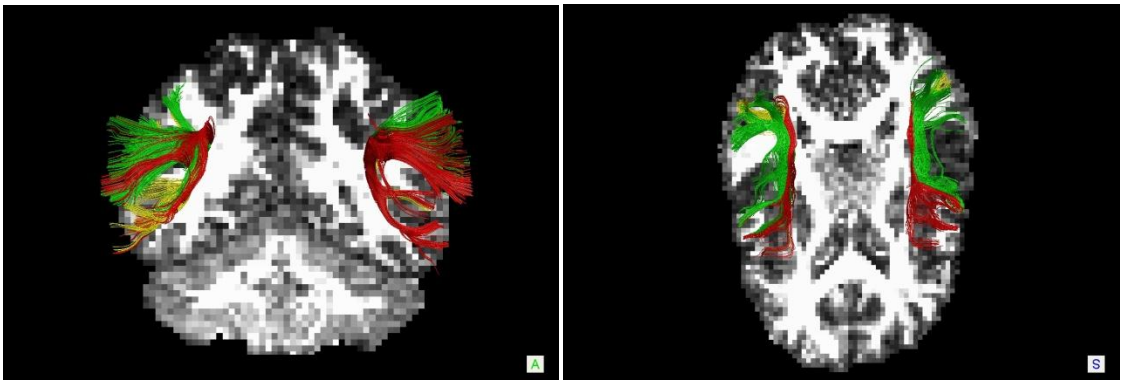

3.2.5.2 Cingulate bundle (see Figure2)

Identification on the color maps: The most dorsal fibers of the cingulum have an antero-posterior course and are easy to identify as green fibers medial to the red fibers of the corpus callosum (MNI 43 to 39). When the left and right halves of the corpus callosum join at the midsagittal line, the cingulum separates into an anterior frontal and a posterior parieto-occipital branch (MNI 37 to 29). The two branches of the cingulum continue to run close to the corpus callosum, turning from green to blue as they arch around the genu, anteriorly (MNI 27 to 1), and the lenium, posteriorly (MNI 27 to 11). The posterior branchcontinues downwards into the parahippocampal gyrus to terminate in the anterior part of the medial temporal lobe.

Delineation of the ROI on the FA maps: A single ROI (Ci) on approximately 30 axial slices is used to dissect the cingulum. A single cigar-shaped region is defined on the top three slices (MNI 43 to 39). When the cingulum separates into two branches an anterior (MNI 37 to 1) and posterior (MNI 37 to L13) region is defined on each slice. It is important to remember that the majority of the fibers of the cingulum are short U-shaped fibers connecting adjacent gyri. The use of a two-ROIs approach excludes the majority of these short fibers from the analysis. For this reason the use of one-ROI approach, which includes all fibers of the cingulum is recommended.

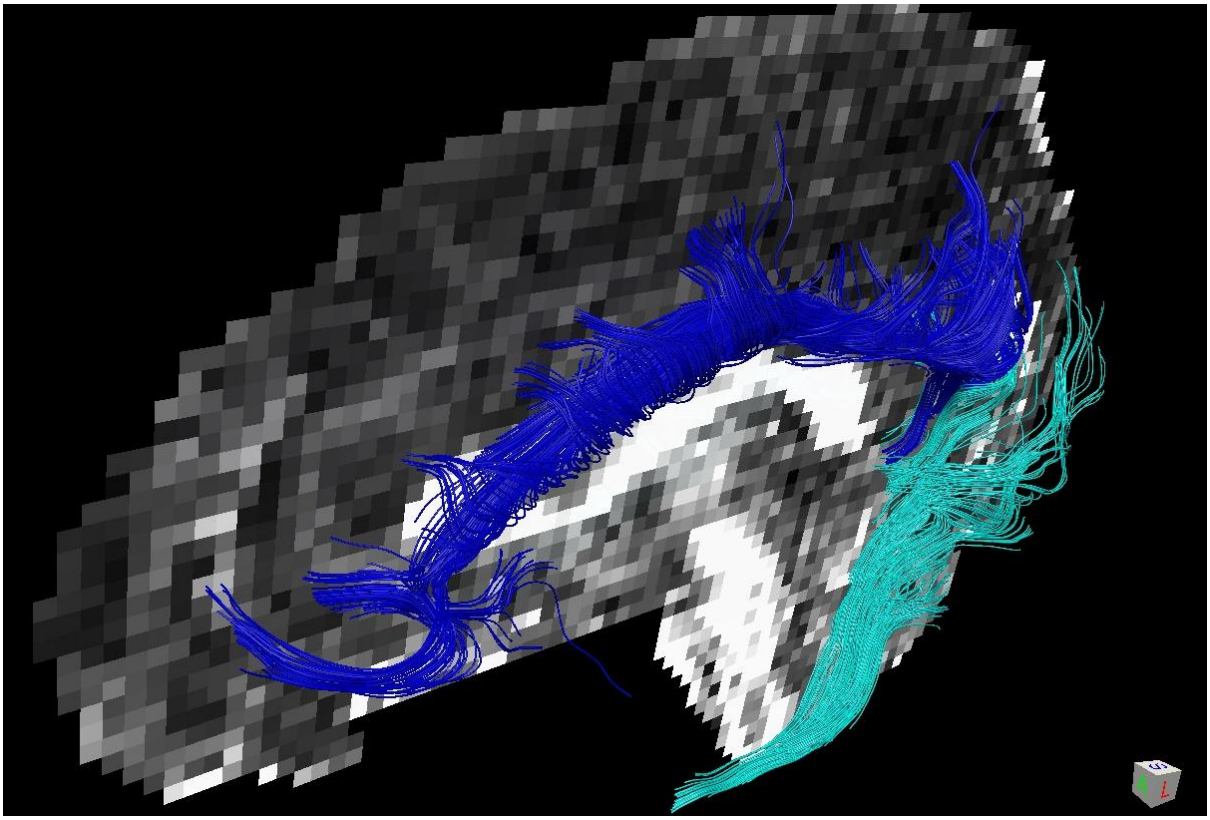

Figure 3.2. The anterior segment of the cingolum (dark blue) and the posterior one (light blue).

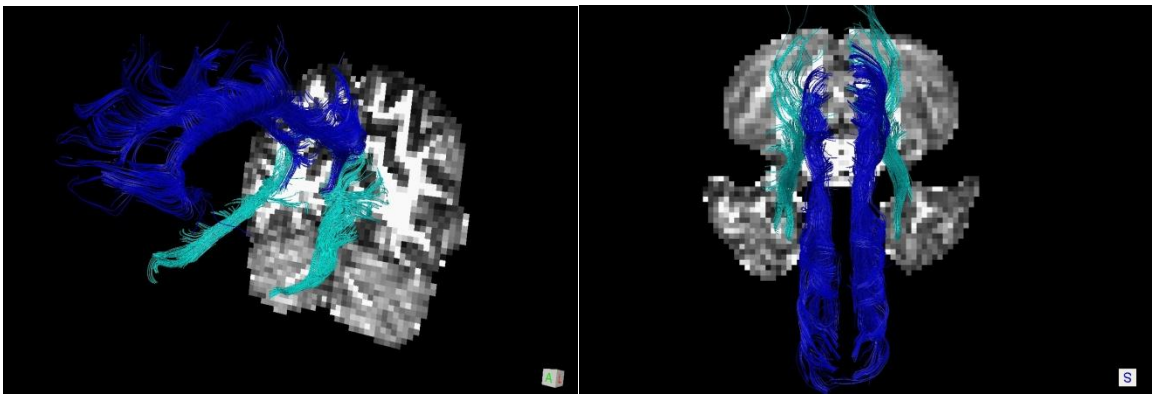

3.2.5.3 Uncinate fasciculus

Identification on the color maps: The temporal fibers of the uncinate fasciculus (red–blue) are medial and anterior to the green fibers of the inferior longitudinal fasciculus (MNI L19 to L11). As the uncinate fasciculus enters the external capsule

(MNI L9), its fibers arch forward (turning from red–blue into green) and mix with the fibers of the inferior fronto-occipital fasciculus.

Delineation of the ROIs on the FA maps: A two-ROIs approach is used to dissect the uncinate fasciculus. The first ROI (temporal, T) is defined in the anterior temporal lobe (MNI L15 to L19), as described for the inferior longitudinal fasciculus. A second ROI (external/extreme capsule, E) is defined around the white matter of the anterior floor of the external/extreme capsule, usually on five axial slices (MNI 1 to L7). The insula defines the lateral border of the ROI, the lenticular nucleus its medial border.

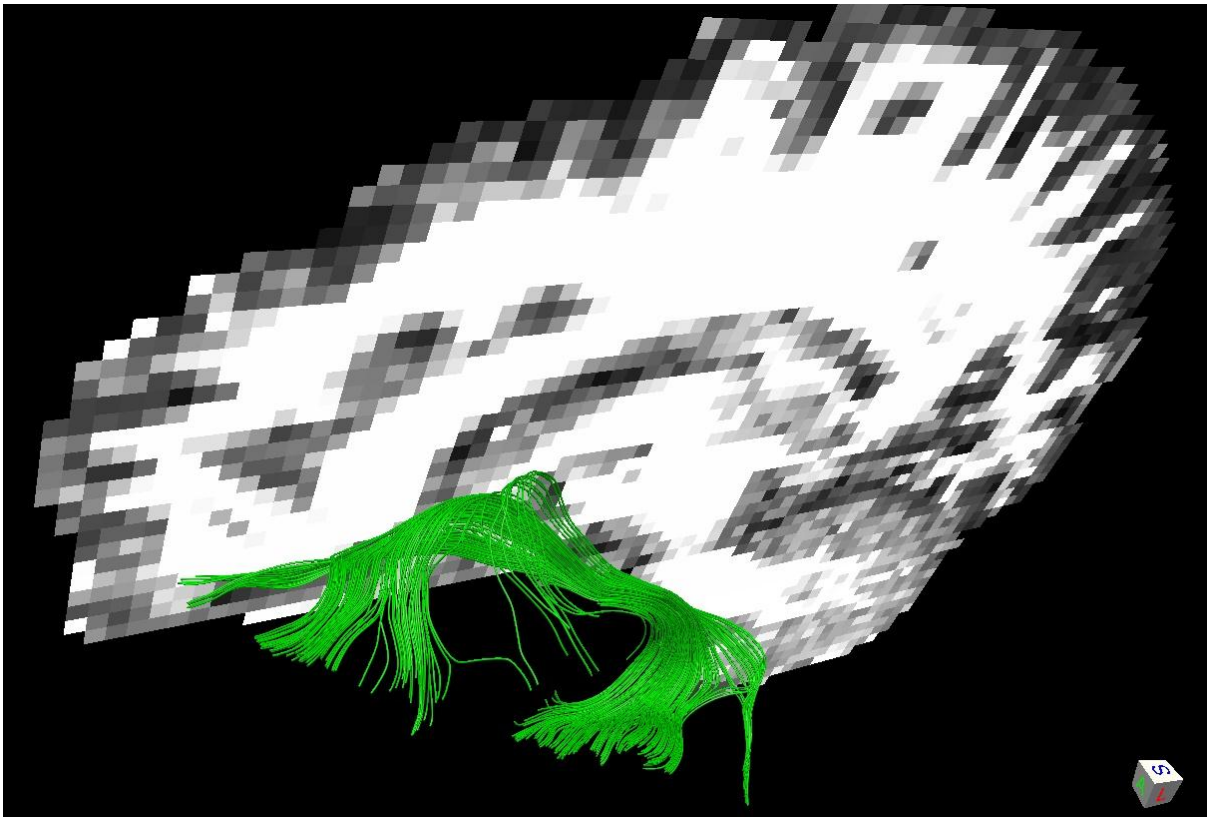

Figure 3.3: Uncinate fasciculus.

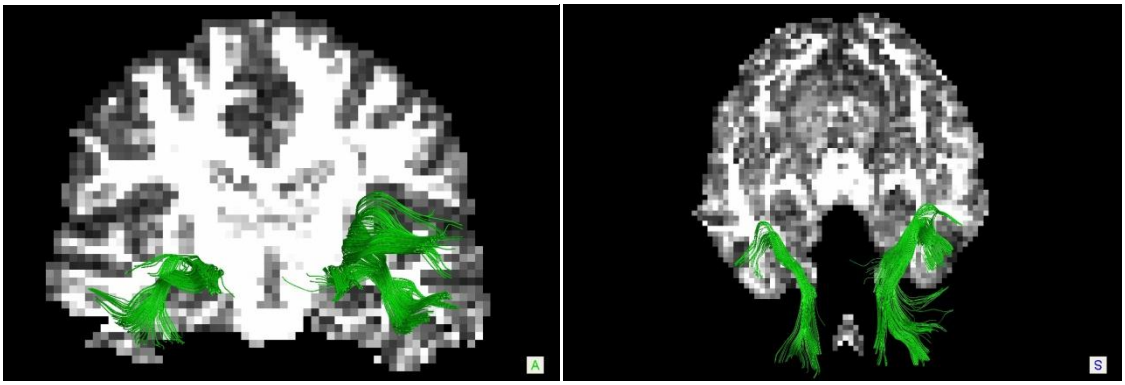

3.2.6 Estimation of Lateralisation Index

At the termination of tracking, the number of reconstructed pathways and the fractional anisotropy, which quantifies the directionality of diffusion on a scale from zero (when diffusion is totally random) to one (when water molecules are able to diffuse along one direction only), was sampled at regular (0.5- mm) intervals along the tract and the means computed. For each reconstructed segment, a lateralisation index (LI) was calculated according to the following formula (*N.*, number):

$$\frac{(N.streamlines\ left) - (N.streamlines\ right)}{[(N.streamlines\ left) + (streamlines\ right)]}$$

Positive values of the index indicate a greater number of streamlines in the left direct segment compared with the right. Values around the zero indicate a similar number of streamlines between left and right. Similarly, a lateralisation index was calculated for the fractional anisotropy and streamlines values of each segment.

3.3 Statistical analyses

Statistical analyses were conducted using SPSS version 16.0 (SPSS inc. Chicago, Illinois, USA).

Subjects were clustered into three groups on the basis of the left-right distribution of the reconstructed pathways of the direct segment using a *k*-means cluster analysis. Whilst X^2 (or Fisher's exact test) was utilized to assess the distribution of the lateralisation index across the participants and between genders, one-sample *t* test (test value _ 0) was used to assess the lateralisation of the index of the fractional anisotropy and of the streamlines values, and two-way ANOVA for between-genders differences.

Also, correlation analysis was performed between the lateralisation index of the direct segment (streamlines) and the neuropsychological performances. Moreover, correlation analysis was performed between tract-specific measurements of fractional anisotropy and neuropsychological performances and ANOVA was used to account for gender differences in neuropsychological performances.

3.4 Results

Using the method described above, we first obtained DT-MRI scans of 24 healthy volunteers (*N* = 23, 11 females) and then we visualized by DT-MRI tractography the different pathways both in the left and right hemisphere. The subjects had been in education for a conspicuous number of years (see Table 3.1).

All participants were right-handed, as assessed using the Lateral Preference Inventory (Coren, 1993a).

Table 3.1. Demographic and clinical variable

	Group (*N* = 23)
Age (years)	24.22 (4.274)
N Male/Female	12/11
Years of Education	15.1304
IQ	108.8261 (10.13837)
CVLT_Immediate Free Recall 1_5	56.6522 (10.89874)
CVLT_Delayed Free Recall_Short Delay	.3913 (.81124)
CVLT_Delayed Free Recall_Long Delay	.2826 (.73587)

3.4.1 Lateralisation index

A lateralisation index (LI) was calculated by counting the streamlines within the long segment of the arcuate fasciculus for each hemisphere. To facilitate a visual representation of the heterogeneous distribution, a k-means cluster analysis was performed to broadly classify the data sets into three groups. This procedure makes no assumptions about underlying differences between individuals but attempts to objectively identify relatively homogeneous groups of cases. The cluster analysis evidenced that 60.9% (14/23) of the subjects showed a leftward asymmetry but with some representation of the right direct segment in the reconstructed tract; thus they had a bilateral but leftward asymmetric distribution (Group 1, left bilateral). Only 17.4% of the subjects (4/23) had a similar left-right distribution; thus they had symmetrical distribution (Group 2, symmetrical bilateral). Another 21.7%of the subjects (5/23) showed a strong left lateralisation of the direct segment (Group 3,

left strong). In the majority of the subject of the strong left group (3/5) it was not possible to reconstruct a continuous trajectory of the corresponding long direct segment connecting Broca's and Wernicke's areas in the left hemisphere. The right hemisphere corresponding segments of the posterior segment of the arcuate fasciculus were present in all the subjects, while the anterior segment in the left hemisphere was absent in two subjects, one for each of the two groups with leftward and symmetric distribution.

Similarly, a lateralisation index was calculated for the fractional anisotropy and streamlines values of each segment.

One-sample *t* test (test value = 0) used to assess the lateralisation of the index of the fractional anisotropy and of the streamlines values evidences several significant interhemispheric differences in all the 3 dissected tracts (Tables 3.2 to 3.5). In the case of the arcuate fasciculus, the FA values of the long direct segment (left, 0.521 ± 0.022; right, 0.499 ± 0.024; $P = 0.000$) showed a significant difference, witht the FA value in the left hemisphere greater than the one in the right. Significant leftward interhemispheric differences in the arcuate were also found in the number of streamlines of the posterior segment (left, 120.87 ± 75.875; right, 108.52 ± 41.257; $P = 0.000$). In contrast, the streamlines of the anterior indirect segment evidenced a significant rightward asymmetry (left, 0.496 ± 0.257; right, 0.510 ± 0.305; $P = 0.004$).

Regarding the cingulate bundle, a significant leftward lateralisation was found both in the dorsal and in the ventral segments. The former showed an interhemispheric significant difference in the FA value (left, 0.502 ± 0.026; right, 0.477 ± 0.020; $P = 0.000$), while the latter in the SL value, although to a lesser degree (left, 200.08 ± 35.121; right, 190.30 ± 35.762; $P = 0.023$). Finally, a significant rightward

lateralisation was found in the FA of the uncinate fasciculus (left, 0.457 ± 0.023; right, 0.478 ± 0.023; $P = 0.000$).

Table 3.1. Mean and standard deviation of fractional anisotropy and streamlines of arcuate fasciculus, cingulate bundle and uncinate fasciculus

Tract	Segment	FA mean (DS)		SL mean (DS)	
		Left	Right	Left	Right
Arcuate fasciculus	anterior	.49685 (.02575)	.51077 (.03050)	91.70 (68.855)	149.52 (83.328)
	long	.52197 (.02243)	.49958 (.02498)	162.48 (73.158)	79.13 (59.846)
	posterior	.47013 (.02794)	.47711 (.02241)	120.87 (75.875)	108.52 (41.257)
Cingulate bundle	dorsal	.50223 (.02646)	.47779 (.02018)	417.04 (105.11)	366.04 (75.750)
	ventral	.43764 (.01778)	.43568 (.01856)	200.08 (35.121)	190.30 (35.762)
Uncinate fasciculus		.45700 (.02306)	.478642 (.02489)	117.65 (52.787)	139.78 (58.113)

Table 2.3. One sample t test assessing the lateralisation of the index of the fractional anisotropy and streamlines values in the three segments of the arcuate fasciculus.

	Test Value = 0						
Arcuate Fasciculus	***N***	**t**	**df**	**Sig. (2-tailed)**	**Mean Difference**	**95% Confidence Interval of the Difference**	
						Lower	**Upper**
LI **FA** Anterior	21	-1.765	20	.093	-.00697	-.0152	.0013
LI **FA** Long	20	5.459	19	<.001	.01299	.0080	.0180
LI **FA** Post	23	-1.231	22	.231	-.00383	-.0103	.0026
LI **SL** Anterior	23	-3.200	22	.004	-.14705	-.2424	-.0517
LI **SL** Long	23	.260	22	.797	.00810	-.0564	.0726
LI **SL** Post	23	6.591	22	<.001	.22323	.1530	.2935

Table 3.3. One sample t test assessing the lateralisation of the index of the fractional anisotropy and streamlines values in the two segments of the cingulated bundle.

		Test Value = 0					
Cingulate Bundle	***N***	**t**	**df**	**Sig. (2-tailed)**	**Mean Difference**	**95% Confidence Interval of the Difference**	
						Lower	**Upper**
LI **FA** Dorsal	23	7.505	22	.000	.01235	.0089	.0158
LI **FA** Ventral	23	.657	22	.518	.00114	-.0025	.0047
LI **SL** Dorsal	23	1.310	22	.204	.01245	-.0073	.0322
LI **SL** Ventral	23	2.435	22	.023	.03050	.0045	.0565

Table 3.4. One sample t test assessing the lateralisation of the index of the fractional anisotropy and streamlines values in the uncinate fasciculus.

		Test Value = 0					
Uncinate Fasciculus	***N***	**t**	**df**	**Sig. (2-tailed)**	**Mean Difference**	**95% Confidence Interval of the Difference**	
						Lower	**Upper**
LI **FA** Uncinate	23	-4.134	22	.000	-.01153	-.0173	-.0057
LI **SL** Uncinate	23	-1.827	22	.081	-.04894	-.1045	.0066

3.4.2 Gender differences in the lateralisation pattern.

Fischer exact test was performed to assess the distribution of the lateralisation index between the two genders. The analysis did not show any significant difference (Table 3.6).

Table 3.5. Expected and actual distribution of the lateralisation index across the subjects and between genders. X2 Tests (or Fischer's exact test).

Clusters		Gender M	Gender F	Total
Left bilateral	Count	4	3	7
	Expected Count	3.9	3.2	7.0
Symmetrical bilateral	Count	5	5	10
	Expected Count	5.5	4.5	10.0
Left strong	Count	2	1	3
	Expected Count	1.7	1.4	3.0

X^2 Tests	Value	Df	Asymp. Sig. (2-sided)
Pearson Chi-Square	.279[a]	2	.870
Likelihood Ratio	.283	2	.868
Linear-by-Linear Association	.017	1	.897
N of Valid Cases	20		

Segments	Males	Females	*P* values
FA Anterior indirect	-.0055 (0.2947)	-.0083 (.01653)	.727

FA Posterior indirect	-.0036 (.01771)	-.0040 (.01205)	.952
FA Long direct	.0137 (.00974)	.0121 (.01220)	.752
SL Long direct	.2121 (.16522)	.2354 (16641)	.739

3.4.3 LI and behavioural correlates

Correlation analysis was carried out between the lateralisation index of the direct segment (streamlines) and the neuropsychological performances. Moreover, correlation analysis was carried out between tract-specific measurements of fractional anisotropy and neuropsychological performance. No significant correlations ($p>0.05$) were found between the neuropsychological performances at both the CVLT and verbal fluency (phonetic and semantic), and the tracts measurements of LI, FA or SL.

3.5 Discussion

Previous studies illustrated a direct correspondence between the anatomy of white matter pathways dissected with DT-MRI tractography and obtained from post-mortem studies (Catani, et al., 2002; Wakana et al., 2007).

Consistently with previous studies, the main finding of the present study is a significant leftward asymmetry in the FA value of the long direct segment of the arcuate fasciculus. Greater FA values in the arcuate fasciculus compared with the corresponding white matter tract in the right hemisphere have been reported previous in several studies (Barrick, et al., 2007; Buchel, et al., 2004; Catani, et al., 2007; Powell, et al., 2006). In addition, we found another significant leftward

lateralisation in the SL of the posterior segment and a rightward distribution of the SL index of the anterior segment of the arcuate fasciculus. To our knowledge only Catani (Catani, et al., 2007) studied the lateralisation of the arcuate fasciculus as dissected into the long direct pathway and the two indirect pathways, anterior and posterior. In contrast with the present results, they found a leftward distribution both of the FA value of the anterior and the posterior segments.

In addition, I found no evidence of a significant relationship between the leftward lateralisation indexes and any measures of language and verbal memory performance in my group. Although counterintuitive, this seems to be in line with the findings of previous DTI (Catani, et al., 2007), showing that the degree of leftward lateralisation of perisylvian pathways might not be correlated with measures of language processing skills, while a more symmetrical FA values might favour the retrieval of verbal material.

One possibility is that the linguistic tasks we have employed might not be specific to any single anatomical structure. For instance, verbal fluency seems to be associated with lesions of anatomical connection between lateral to medial frontal cortex and the head of caudate, a network that is not comprised in the perisylvian circuitry.

We also investigated the lateralisation distribution of FA and SL values of other pathways for completeness, in order to compare the hemispheric organisation of the arcuate fasciculus with the organisation of other white matter tracts.

The cingulate bundle showed a significant leftward asymmetry. More specifically, we found a significant leftward distribution of the FA index in the dorsal segment and a significant asymmetry going in the same direction in the number of streamlines in the ventral segment. Although not many studies investigated the lateralisation of the cingulate bundle white matter fibres in healthy subjects, our result of a greater FA in

dorsal segment for the left hemisphere are consistent with all the previous findings (de Groot et al., 2009; Gong et al., 2005; Malykhin, Concha, Seres, Beaulieu, & Coupland, 2008).

In addition, we found a significant rightward distribution of FA values in the uncinate fasciculus which is consistent with the results reported by all the previous studies that explored this white matter pathway in healthy subjects (Malykhin, et al., 2008; Yasmin et al., 2009) .

Taken together, these results replicate the previous findings and indicate that the leftward lateralisation is not exclusive of the arcuate fasciculus, but other tracts like the cingulate bundle may show the same hemispheric asymmetry.

Unlike some of the previous studies (Kang, Herron, & Woods, 2011; Y. Liu et al., 2011), we did not find any significant difference in the lateralisation of the arcuate between the two genders. This result may be due to the small sample, which did not allow an examination of gender differences with high statistical power.

At present, DT-MRI tractography is the only non-invasive method that allows the large pathways of human brain white matter in vivo (Le Bihan, 2003). Nonetheless, it is important to remember that DT-MRI measures the diffusion of water molecules and that the computed tractography lines are only interpreted as fibre tracts. As a consequence, there is a statistical uncertainty in the tract results. DT-MRI provides only indirect measurements of tissue; hence there is no certain correspondence between tractography indices and underlying biological factor.

4. INVESTIGATING LATERALISATION IN THE LANGUAGE NETWORK: A FUNCTIONAL CONNECTIVITY STUDY

4.1 Introduction

A fundamental characteristic of human brain organisation is the existence of functional and structural asymmetries between the hemispheres (Geschwin.N & Levitsky, 1968; Geschwind & Galaburda, 1985). Cerebral asymmetry is observed early in the human brain. The normal infant brain is already asymmetrically organised during the first months of life (Dehaene & Dehaene-Lambertz, 2009). The exact determinants of this process of lateralisation remain mostly unknown, but the centrality of cerebral and behavioural asymmetries converges on a possible human laterality gene. A leading hypothesis in this regard suggests that a dominant allele known as the 'right-shift' factor is responsible for establishing left cerebral asymmetry by disrupting the development of language related abilities of the right hemisphere during childhood (Annett, 2002).

Studies on patient and non-patient populations have repeatedly shown that the left and right hemispheres (LHem and RHem) can be different in their structures (e.g. size, location, and/or shape of different areas) and in their information processing faculties (Cabeza & Nyberg, 2000; Gazzaniga, 2000).

One of the most studied and earliest observed lateralised brain functions is language.

Superior temporal (Wernicke's area) and inferior frontal (Broca's area) areas in the left hemisphere have been classically associated with language comprehension and production.

However, lesion (Dronkers, Wilkins, Van Valin, Redfern, & Jaeger, 2004) and functional magnetic resonance imaging (fMRI) studies (Price, 2010) have identified additional temporal, parietal and prefrontal regions, supporting the involvement of a more extended language network (M. M. Mesulam, 1990; A. U. Turken & Dronkers, 2011). This network seems to be organised around a central axis of at least two interconnected heteromodal epicenters (Wernicke's and Broca's areas) (M. Mesulam, 2005) and abnormalities in its flexible parallel architecture might help explain various clinical manifestations in language disorders (aphasia) (Catani, et al., 2005). Wernicke's area (Brodmann areas, BAs, 22, 39 and 40) is traditionally associated with language comprehension and its damage results in Wernicke's aphasia (receptive or fluent aphasia). Broca's area (posterior inferior frontal gyrus; BA 45 and 44) is traditionally associated with language production, and its damage results in Broca's aphasia (expressive or non-fluent or agrammatic aphasia).

Lesion and fMRI studies in healthy subjects have indicated that speech comprehension and production are lateralised to the left brain hemisphere (A. U. Turken & Dronkers, 2011).

In the most recent study, using a large resting-state functional connectivity and lesion studies from 970 healthy subjects and seed regions in Broca's and Wernicke's, Tomasi & Volkow (2012) reported that Analysis of laterality patterns revealed a leftward lateralisation for the long-range connectivity in Broca's area and in posterior Wernicke's (angular gyrus), which is consistent with previous resting state functional connectivity studies (H. Liu, Stufflebeam, Sepulcre, Hedden, & Buckner, 2009) and supports lateralisation of language to the left hemisphere. However, the authors also documented an unexpected rightward lateralisation of the anterior Wernicke's region for long-range connectivity that suggests a predominant

involvement of the right hemisphere in language comprehension processed through the supramarginal gyrus . Resting state functional connectivity MRI can reveal the cortical connectivity among language-network regions by evaluating correlations of spontaneous BOLD signal-intensity fluctuations (Biswal, Yetkin, Haughton, & Hyde, 1995; Fox et al., 2005).

However, there are no functional connectivity MRI studies that directly investigate language lateralisation in healthy subjects. The majority of them focused either on a specific population of patients (schizophrenic, epileptic, etc.)(Bleich-Cohen et al., 2012) or on a specific aspect of language (reading, comprehension, production, phonology, semantics, etc.) (Seghier & Price, 2010; van Atteveldt, Roebroeck, & Goebel, 2009; Xiang, Fonteijn, Norris, & Hagoort, 2010). Nevertheless, healthy subjects have been used as control in order to draw conclusions in studies on a specific disorder (Bleich-Cohen, et al., 2012; Pravata et al., 2011). This is the first study to investigate front-temporal connectivity in healthy patients using the Hayling Sentence Completion Test.

The following hypotheses were tested:

1) A leftward hemispheric asymmetry would be found in the blood oxygenation level-dependent response across all conditions.
2) All the correlations between paired ROIs would be significantly different from zero and they would be all positive.
3) A leftward hemispheric asymmetry would be found in the lateralisation index calculated on the correlation values of the paired ROIs in the functional connectivity analysi

4.2 Methods

4.2.1 Participants

Twenty-three healthy male (n=12) and female (n=11) without any current or previous evidence of psychiatric disorders recruited through advertisement from the local South London community. All but one subject were right-handed, while English was the first and native language of all the participants in this study. The acquisition period for this study lasted about 15 months. See Chapter 2 for a detailed description of the demographic characteristics of the subjects and the inclusion/exclusion criteria.

However, after pre-processing of the fMRI images one of the male volunteers was removed on the basis of excessive head movements (i.e. head translation parameters > 10 mm and head rotations parameters > 1 degree) inside the scanner, leaving scans from 22 healthy controls for the subsequent analysis. The additional exclusion criteria for the healthy controls are reported in detail in Chapter 2, section 2.1. See Table 1 for the demographic characteristics of this sample.

4.2.2 Functional MRI task design

In this study subject performed a modified version of the Hayling Sentence Completion Task (HSCT) that was initially described by Burgess and Shallice (1996). The HSCT allows the examination of verbal initiation and suppression skills while maintaining changes in the characteristics of the two component of the task to the minimum. Subjects are presented with sentence stems in which the last word is omitted. In one condition, referred here as response Initiation, the subject has to complete the sentence with a word which is semantically related with the context of

the sentence. In another condition, referred here as response Suppression, the subject has to provide a word which is not semantically related to the sentence stem and does not make sense in its context. Therefore, in this condition the most obvious response must be inhibited. Previous behavioural studies showed that both patients with frontal lesions and chronic psychotic patients perform the HSCT task poorly (Burgess & Shallice, 1996; Nathaniel-James & Frith, 1996). More recently, Nathaniel-James and colleagues (2002) devised a second version of the HSCT in which activity associated with selection between different correct words could be distinguished from activity associated with suppression of a prepotent response. This was achieved by varying the contextual constraint of the sentences from high to low. The contextual constraint of a sentence can be quantified in terms of close probability (CP), which represents the probability that a particular word will be used to complete the sentence. It follows that the lower the CP of a sentence the larger the number of potential correct words that become available (Nathaniel-James & Frith, 2002).

The version used in the present research is a modification of the HSCT that was implemented in order to adapt the task to a fMRI experiment (Allen et al., 2008). Eighty sentences were selected from those provided by Arcuri and colleagues (2001) and Bloom and Fischler (1980). Sentences were chosen on the basis of having a high probability of one completion (high-constraint sentences: $CP > 0.9$) or a low probability of one particular response (low-constraint sentences: $CP < 0.3$). Sentence stems consisted of five, six or seven words and were assigned to either a response Initiation condition, in which participants were required to provide a congruent response (i.e., 'He posted the letter without a STAMP'), or a response Suppression condition, in which participants had to complete the sentence with an

incongruent condition (i.e., 'The boy went to an expensive SHOE'). In addition, the experimental paradigm comprised of a control condition, referred here as Repetition, in which participants were presented with the word "REST" and were instructed to read it overtly. The sentences assigned to each congruency condition were matched for word length (equal number of 5, 6 and 7 words) and constraint (equal number of high and low CP sentences). The experimental design consisted, therefore, of a 2-by-2 factorial structure, with congruency (Initiation and Suppression) and constraint (high CP and low CP) as factors.

4.2.3 fMRI procedure

The 40 sentence stems assigned to each congruency condition were arranged into blocks, which contained five sentence stems each. The two conditions (i.e. Initiation and Suppression) were presented in two separate acquisition sessions. Within each condition, the level of constraint was alternated between each block in an ABABABAB design. To control for the effects of inter-subject reading speed, each word was presented visually in the MRI scanner one at a time at an interval of 500ms. The words appeared form right to left and all words in the sentence stem remained on the screen together for a further 500ms after the last word of the stem had appeared. Subsequently, a question mark appeared which cued participants to articulate their verbal response. The question mark remained for a further 4 sec in which time a response was made before the first word of the next stem was presented. Therefore, each block of 5 sentences lasted for 40 sec with a total inter-stimulus interval of 8 sec between the presentations of each sentence stem. The experimental conditions were contrasted with a control condition consisting of a

cross that was presented for 4 sec and was followed by the word “REST”, which participants had to articulate overtly, for a further 4 sec. As for the sentences, the control trails were arranged into blocks which contained 5 trails each and lasted 40 sec. Therefore, within each session an experimental block (E) was alternated with a control block (C) in an ECECECECECECECE design for a total of 8 experimental blocks and 7 control blocks per session.

Participants were trained before scanning with sentence stems different to the ones included in the fMRI task. None of the participants reported difficulties in reading any sentence stem in the allotted presentation time. Once inside the scanner, subjects were asked to listen to a standardised instruction communication before the response Initiation phase and again before the response Suppression phase of the task.

An audio software (Cool Edit Synthtrilium) for the analysis of error rates and response times was used to record the participants’ overt verbal responses. The latency between the presentations of the question mark and the onset of the participants’ verbal response was measured by using a software-based voice trigger. During the acquisition of dummy volumes before each of the two functional runs, the average power spectrum of the scanner noise was computed and set as a noise profile. This profile was then applied to digitally filter the microphone input signal by using a non-linear subtraction method and band-pass filtering of the highest amplitude frequencies. Consequently, the root mean square (RMS) value of 8-msec epochs of the differential of the filtered signal was then calculated. Speech onset was determined when the RMS value exceeded a preset threshold set at just above scanner noise with no voice component.

4.2.4 fMRI Data Acquisition

Images were acquired on a 3.0T GE Signa system (GE Medical Systems, Milwaukee) using a TR of 2 seconds, flip angle of 70°, TE of 30 ms, slice thickness of 3mm, interslice gap of 0.3mm and field of view 240 mm. A total of 600 image volumes were acquired for each subject in two runs (300 Initiation and 300 Suppression), each run acquisition lasting 10 minutes. For each subject, 38 axial slices parallel to the AC-PC line were acquired with an image matrix of 64×64 (Read×Phase) providing whole-brain coverage.

The use of overt verbal responses in the absence of a clustered or compressed fMRI acquisition could potentially raise concerns regarding movement artifacts due to response articulation (Barch et al., 1999). These potential concerns were addressed by: (i) defining the primary comparisons between conditions that both (Initiation/Suppression and Repetition) implied overt verbal responses, and (ii) performing the statistical analyses on pooled group data rather than individual participant data (Allen, et al., 2008). Moreover, this version of the HSCT has been previously used in the absence of a cluster acquisition and movement artifatcs due to articulation were not observed (Allen, et al., 2008; Allen et al., 2010). In the present acquisition, only one healthy control showed significantly greater head translations and rotations parameters (see Healthy Controls section above) and was therefore removed from the subsequent analyses.

4.2.5 Behavioural Analysis

In the Initiation condition errors occurred when participants gave no response or a response that did not make sense in the context of the preceding sentence stem. In

the Suppression condition errors occurred when participants gave no response or a response that completed the preceding sentence stem in a sensible way. The validity of each completion in the Suppression condition was defined in accordance with the Hayling and Brixton Test section 5 (Thames Valley Test Company Ltd, 1997). When there was uncertainty as to the appropriateness of a response a consensus decision was made between two investigators. A repeated measure ANOVA with congruency and constraint as within-subject factors (version 19.0, IBM Comp. & SPSS Inc., 2010) to analyse mean errors proportions and reaction times.

4.2.6 Functional MRI data analysis

Pre-processing and statistical analysis of functional data were performed in SPM8 software (http//www.fil.ion.ucl.ac.uk/spm), running in Matlab 10 (Matworks Inc.Sherbon, MA, USA).

Pre-processing. For each subject, a limited number of image volumes were randomly selected for visual inspection of potential image artifacts.

After visual inspection, the first image of the Suppression run was realigned to the first image of the Initiation run; then all image volumes from each run were realigned to the first image of the corresponding run and resliced with sync interpolation. The realigned images were spatially normalised to a standard MNI-305 template (K. J. Friston, Frith, Frackowiak, & Turner, 1995) using nonlinear-basis functions. As a final step, the normalised functional images were convolved by a 6mm full width at half maximum (FWHM) isotropic Gaussian kernel in order to compensate for residual variability in functional anatomy after spatial normalisation as well as to permit application of Gaussian random field theory-based procedures

for adjusted statistical inference. More details on the pre-processing can be found in Chapter 2, section 2.3.

Statistical Parametric Mapping. A standard voxel-wise statistical analysis of regional responses, implemented in accordance to the General Linear Model (GLM) statistical framework, was performed in order to identify regional activations in subject independently. To remove low-frequency drifts, the data were high-pass filtered using a set of cosine basis functions with a cut-off period of 128s. The two sessions (Initiation and Suppression) were modelled separately to control for session-specific confounding effects on the regional activations. For the Initiation session, the following experimental conditions were modelled: Initiation (High CP), Initiation (Low CP), Reading, Repetition, Fixation; for the Suppression session, the following experimental conditions were modelled: Suppression (High CP), Suppression (Low CP), Reading, Repetition, Fixation. The above conditions were modelled in an event-related fashion by convolving the onset times (e.g. the onset of the question mark prompting a verbal response) with a canonical haemodynamic response function. In addition, in both sessions error responses were modelled as a separate regressor, which was included in the GLM as a covariate of no interest. Serial correlations among scans were modelled using an AR(1) model, enabling maximum likelihood estimates of the whitened data. The parameter estimates were calculated for all brain voxels using the GLM and contrasts were computed for each condition of interest (i.e. High Initiation vs. Repetition; Low Initiation vs. Repetition; High Suppression vs. Repetition; Low Suppression vs. Repetition). The subject-specific contrast images were then entered into a second-level random effects analysis to make inferences at group level. In order to reduce the confounding effects of inter-subject variability and better investigate the effect of group-by-task interactions, a

repeated-measure ANOVA was implemented in SPM8 by defining a 2×2 flexible factorial design. This design allows the modelling of inter-subject variability by specifying each subject as a separate factor (see Glasher & Gitelman flexible factorial design tutorial, http//www.fil.ion.ucl.ac.uk/spm). However, flexible factorial designs can also potentially overestimate the extent and significance of main effects of condition and group (McLaren et al., 2011). Therefore, in addition to the flexible factorial design mentioned above, a standard 2×2 factorial ANOVA was used to characterise the main effect of congruency, constraint. For both analyses, statistical inferences were made at a whole-brain corrected voxel level ($p<0.05$, FEW corrected, cluster extent threshold = 5).

Table 4.6. Mean and standard deviation for Proportion of Errors and Reaction Times during the HSCT

Condition	Mean Proportion of Errors	Mean Reaction Times
Initiation High CP	.021(.044)	764.33(223.71)
Initiation Low CP	.120(.086)	1145.35(471.39)
Suppression High CP	.0837(.104)	1251.03(568.06)
Suppression Low CP	.161(0.115)	1317.66(659.42)

4.2.6 Functional Connectivity Analysis

In neuroimaging, functional integration between brain areas can be characterised in terms of functional connectivity, which refers to correlation over time between activity in spatially remote brain areas, or effective connectivity, which refers to the influence that the activity in one region exerts over another (Friston 1994).

In the present exploratory study, there were no specific a-priori hypotheses as to the directionality (i.e forward versus backward) of the inter-regional interactions and the impact of the experimental condition on the relationship between structural and functional connectivity within the perisylvian network. Thus an exploratory correlation analysis based on Pearson's correlation coefficient was preferred to a more hypothesis-driven analytical approach (e.g. Dynamic Causal Modelling).

4.2.7 Regions of interest (ROIs) identification

For the purpose of this study, language related lateralisation was examined in a network of regions of interest (ROIs) including: the inferior frontal gyrus [IFG, mean coordinates (x, y, z): –58, 18, 32 (left); (x, y, z): 58, 18, 32 (right)], which represents the Broca's area on the left; the middle temporal gyrus [MTG, mean coordinates (x, y, z): –58, -30, -12 (left); (x, y, z): 58, -30, -12 (right)], which represents the Wernicke's area on the left; and the inferior parietal lobule [IPL, mean coordinates (x, y, z): –47, -59, 40 (left); (x, y, z): 47, -59, 40 (right)], which represents the Geschwind's area. These three areas were used as seed regions the same used to divide the arcuate fasciculus in three segments in the DTI study (chapter 3).

Time-series were therefore extracted from three ROIs: the left inferior frontal gyrus (LIFG), the middle temporal gyrus (LMTG) and the left inferior parietal lobule (Figure 1). These regions have been previously implicated in studies investigating language and semantic processing (Price, 2000b, 2010) and represent the perysilvian network of regions connected through the AF (Catani, et al., 2005). In order to ensure comparability across subjects, the extraction of time series had to meet a combination of anatomical and functional criteria. Functionally, the principal

eigenvariates were extracted to summarise regional responses in 12 mm spheres centred on the ROIs included in the study. To account for individual differences, the location of these regions was based upon the local maxima of the subject-specific statistical parametric maps, defined as the nearest (within 10 mm) of the group maxima. The mean coordinates for the LIFG and LMTG were derived from activation maps obtained with the standard SPM analysis of the HSCT data. The mean coordinates for the LIPL were derived from previous studies which provided evidence of LIPL involvement in semantic processing (Price, 2010). Anatomically, the search for each subject-specific local maximum was constrained within the same correspondent cortical area, as defined by the PickAtlas toolbox (Maldjian, Laurienti, Kraft, & Burdette, 2003b). There were no regions that conformed to these criteria in one subject, which was therefore excluded from this study.

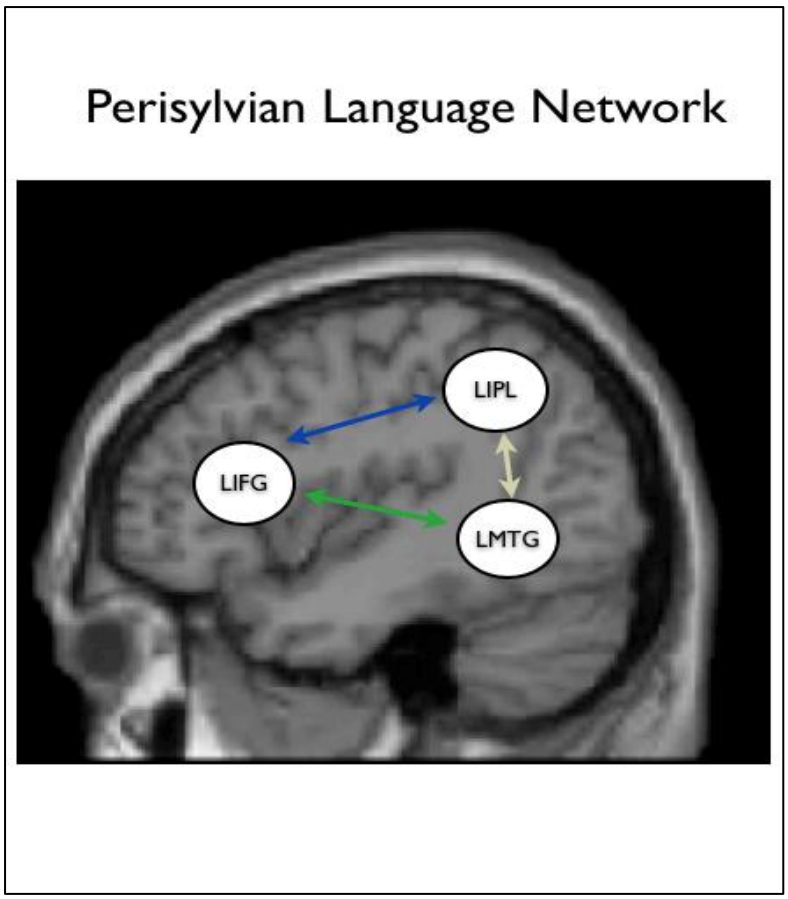

Figure 4.1. ROIs for the extraction of Time Series

4.3 Statistical analysis

Statistical analyses were conducted using SPSS version 16.0 (SPSS inc. Chicago, Illinois, USA).

Pearson's correlation analysis was then performed for each subject between the three ROIs within each hemisphere (LIFG_LMTG, LIFG_LIPL, LMTG_LIPL, RIFG_RMTG, RIFG_RIPL, RMTG_RIPL). Each correlation gives a measure of the connectivity between two areas that are connected by a specific segment of the arcuate fasciculus, as examined in the chapter 3. We assumed that the inferior frontal gyrus (IFG), that corresponds to Broca's area, was connected to the middle temporal gyrus, that corresponds to Wernicke's area, through the long direct

segment of the arcuate fasciculus. So we referred to the IFG-MTG correlation as the long segment. Similarly, we assumed that the IFG was connected to the inferior parietal lobule (IPL), that corresponds to Geschwind's area, through the anterior indirect segment of the arcuate fasciculus. So we referred to the IFG-IPL correlation as the anterior segment. In the end, we assumed that the MTG was connected to the IPL through the posterior indirect segment of the arcuate fasciculus. So we referred to the MTG-IPL correlation as the posterior segment. A one sample *t* Test (test value_0) was then performed on the *obtained Pearson* product-moment correlation *coefficient*s (*r*) for each "tract" (LIFG_LMTG, LIFG_LIPL, etc.). The same coefficients were subsequently used to calculate the Lateralisation index for each "tract" and each subject.

For example:

$$(LI)IFG\_MTG = \frac{(rLIFG\_LMTG) - (rRIFG\_RMTG)}{[(rLIFG\_LMTG) + (rRIFG\_RMTG)]/2}$$

Accordingly, negative value of the LI stands for right lateralisation while positive numbers yielded lateralisation to the left in each subject.

One-sample *t* test (test value _ 0) was used to assess the lateralisation of each "tract".

4.4. Results

4.4.1 Functional MRI

Overal Task Activation

Increased blood oxygenation level-dependent response across all conditions (response Initiation, response Suppression, High- and Low-constraint conditions) compared to Repetition was observed in the left superior frontal gyrus (SFG), the left inferior frontal gyrus (IFG), the left middle temporal gyrus (MTG) and the left thalamus (Figure 4.2; Table 4.1). When the Initiation condition was individually contrasted against Repetition, additional clusters were detected in the left SFG, left Insula and left MTG (Figure 4.3, Table 4.1). Similarly, when Suppression condition was separately contrasted against Repetition, three major clusters were found in the left SFG, left MFG and in the left insula (Figure 4.4, Table 4.1). Finally, when Suppression was contrasted against Initiation, clusters were detected in the right Superior Parietal Lobe, in the right MTG and in the left Cuneus (Figure 4.5, Table 4.1)

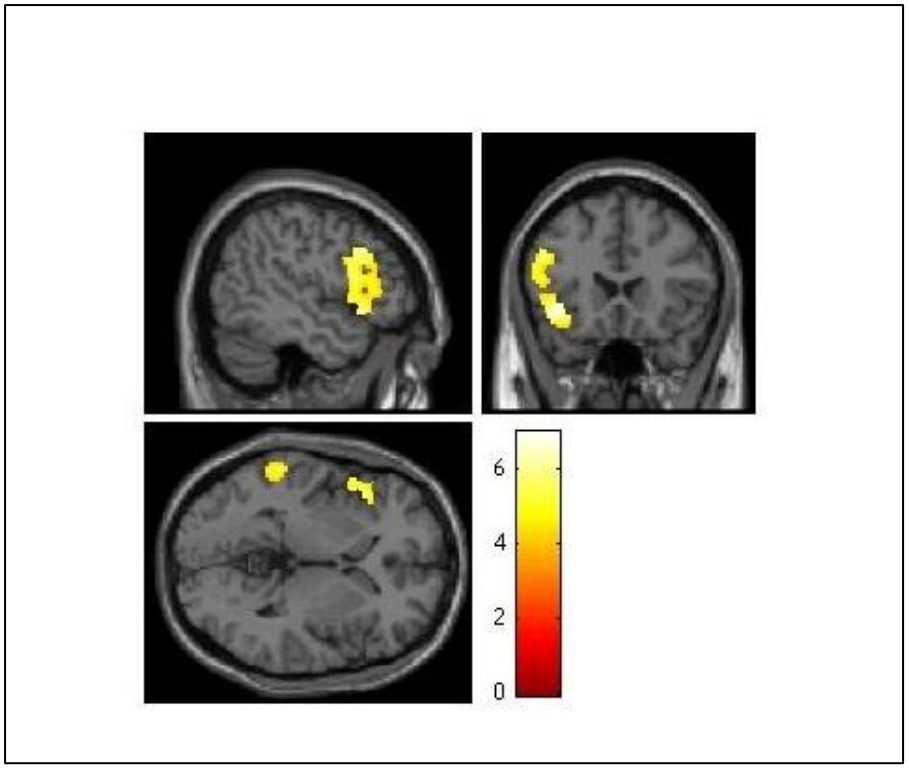

Figura 4.2. Statistical parametric maps showing Initiation & Suppression > Repetition. For visualisation purposes, activations are reported at a whole brian voxel-level uncorrected for multiple comparisons (P<0.001).

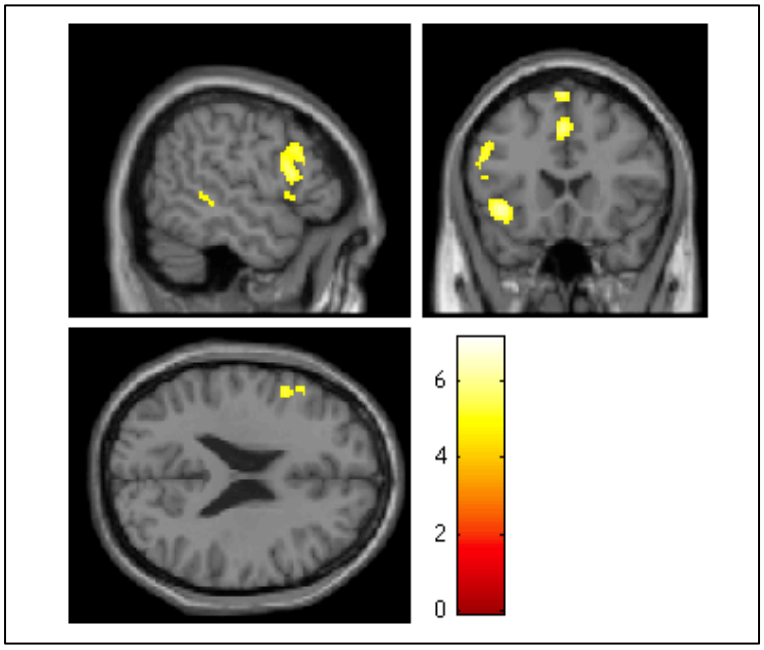

Figura 4.3. Statistical parametric maps showing Initiation > Repetition. For visualisation purposes, activations are reported at a whole brian voxel-level uncorrected for multiple comparisons (P<0.001).

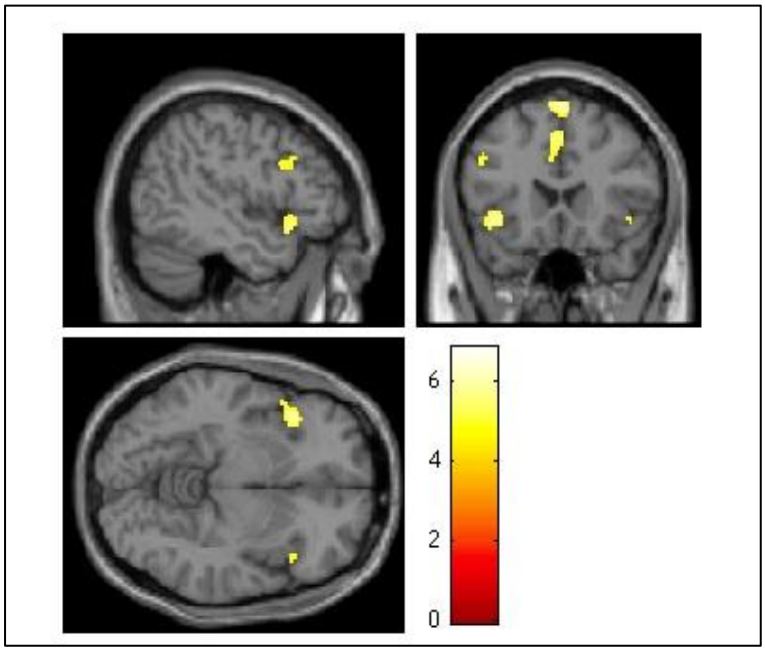

Figura 4.4. Statistical parametric maps showing Suppression > Repetition. For visualisation purposes, activations are reported at a whole brian voxel-level uncorrected for multiple comparisons (P<0.001).

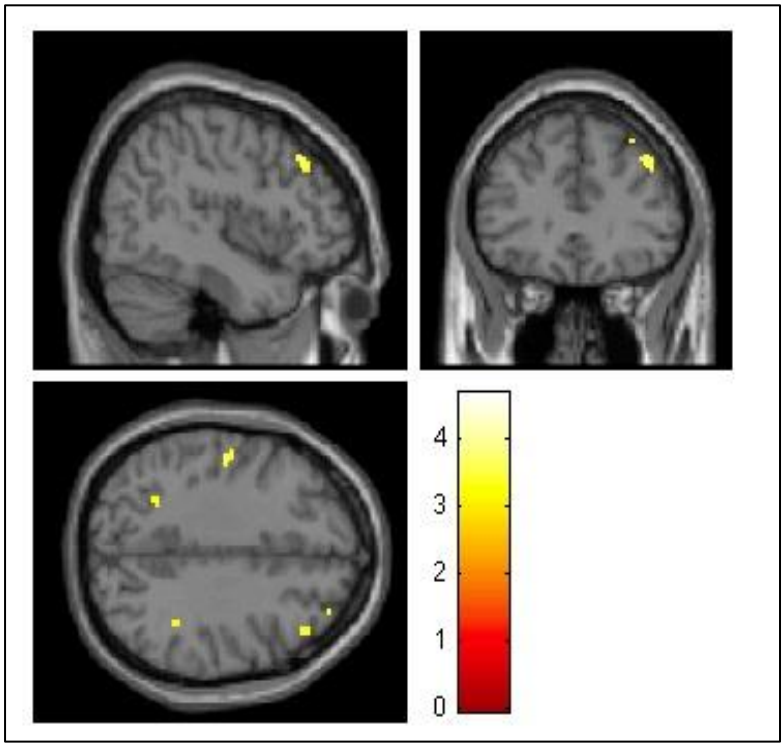

Figura 4.5. Statistical parametric maps showing Suppression > Initiation. For visualisation purposes, activations are reported at a whole brian voxel-level uncorrected for multiple comparisons (P<0.001).

Region	*x*	*y*	*z*	*BA*	*Cluster size*	*Z score*
Initiation & Suppression>Repetition						
L Medial Superior frontal gyrus	-40	22	-6	45	2125	6.66
L Inferior frontal gyrus	-60	-40	0	21	518	4.80
L Middle temporal gyrus	-58	-50	22	40	14	3.60
L Medial Superior frontal gyrus	-40	22	-6	45	2125	6.66
Initiation > Repetition						
L Superior frontal gyrus - SMA	-2	12	60	6	545	6.78
L Insula	-40	22	-6		539	6.02
L Middle temporal gyrus	-58	-40	2	22	124	5.45
Suppression > Repetition						
L Superior frontal gyrus - SMA	-2	12	64	6	687	6.56
L Insula	-40	22	-6		141	5.81
L Middle temporal gyrus	-50	18	30		69	5.05
Suppression > Initiation						
R Superior parietal lobe	8	-70	48		433	4.57
R Middle temporal gyrus	42	30	40		43	3.93
R Middle temporal gyrus	28	56	28	10	28	3.89
L Cuneus	-8	-80	32	19	39	3.85
R Middle temporal gyrus	32	12	64		140	3.82

Table 4.1. Coordinates and Z-scores (voxel-level P<0.05, FWE corrected) for cerebral areas activated during Initiation and Suppression relative to Repetition, and Suppression against Initiaton.

4.4.2 Functional Connectivity

One-sample *t* test (test value = 0), performed on the coefficients of the correlation between the ROI (Table 2), evidenced that all the correlations between paired ROIs

are significantly different from zero and they are all positive. This result supports the hypothesis that there is a strong functional integration within the investigated brain network.

	Test Value = 0						
	N	t	Df	Sig. (2-tailed)	Mean Difference (Std. Deviation)	95% Confidence Interval of the Difference Lower	Upper
LIFG_LIPL	22	8.676	20	p<.001	.3472 (.1833)	.2637555	.4307207
LIFG_LMTG	22	13.460	20	p<.001	.5231 (.1781)	.4420681	.6042176
LMTG_LIPL	22	9.924	20	p<.001	.4200 (.1939)	.3317949	.5083956
RIFG_RIPL	22	9.897	20	p<.001	.4936 (.2285)	.3896222	.5977112
RIFG_RMTG	22	8.186	20	p<.001	.4592 (.2571)	.3422489	.5763225
RMTG_RIPL	22	8.841	20	p<.001	.3409 (.1767)	.2604692	.4213403

Table 4.2. One sample t test assessing that the ROIs coefficients of correlation were significantly different from zero.

One-sample *t* test (test value = 0) was also used to assess the lateralisation index of the in all the 3 investigated tracts (Table 4). The results evidenced that only the anterior connection, between the Broca's and Geschwind's areas, showed a significant rightward lateralisation (left, 0.347 ± 0.183; right, 0.493 ± 0.228; P = 0.037).

Tract	*r* mean (DS)	
	Left	Right
IFG-IPL	.347 (.183)	.493 (.228)
IFG-MTG	.523 (.178)	.459 (.257)
MTG-IPL	.420 (.193)	.340 (.176)

Table 4.3. Mean and standard deviation of Person's r in the three connections in both hemispheres.

	Test Value = 0						
						95% Confidence Interval of the Difference	
	N	t	df	Sig. (2-tailed)	Mean (Std. Deviation)	Upper	Upper
LI_ant	22	-2.232	20	.037	-.09043 (.18569)	-.1750	-.0059
LI_long	22	1.052	20	.305	.64621 (2.81363)	-.6345	1.9270
LI_post	22	.705	20	.489	.03252 (.21142)	-.0637	.1288

Table 4.4. One sample t test assessing the lateralisation of the index of the correlation coefficient in the three tracts.

4.5 Discussion

The HSCT is known to robustly activate left hemisphere frontal and temporal regions. For example, Nathaniel-James (1996) found that when compared with a control reading task, the HSCT is associated with activation in 3 areas, the left frontal Opercolum, the left inferior frontal gyrus and the right anterior cingulate. In addition and more recently, Allen (2008) found that the BOLD response across all conditions

compared to rest was associated with activation in the left superior frontal gyrus, the LMTG, the left ventrolateral inferior frontal gyrus, the left dorsolateral MFG, the left cuneus, and the bilateral superior temporal pole. Consistently with all the previous studies, for sentence completion versus rest, in the present work we found activation in areas commonly associated with self-generated word production tasks, i.e. dorsolateral and medial prefrontal areas and superior/middle temporal gyrus (Frith et al., 1995; Lawrie et al., 2002; Nathaniel-James, Fletcher, & Frith, 1997).

However, whether specific patterns of functional connectivity are associated with the regional activation observed during this task has yet to be elucidated since, to the best of my knowledge, no previous studies have addressed this issue.

In this study I employed a Pearson's correlation analysis to characterise functional connectivity within the perysilvian network and this analytical approach does not allow one to estimate the functional correlation coefficient specific to each task condition (i.e. response Initiation, response Suppression, High- and Low-constraint conditions compared to Repetition). Therefore it is difficult to differentiate the modulation effects of functional connectivity on the basis of the two different performance components. . A more appropriate approach would have been the analysis of effective connectivity of response initiation and suppression which have different neuroanatomical substrates, there is a problem with interpreting performance on complex executive tasks that incorporate both of these components when it is not possible to separate them in the analysis.

The main finding of the fc analysis is a significant rightward lateralisation (left, 0.347 ± 0.183; right, 0.493 ± 0.228; $P = 0.037$) in the anterior connection, between the the IFG and the IPL. The functional connectivity analysis revealed an increase in the strength of inter-regional coupling between the RIFG and RIPL.

In order to comprehend complex, natural language the right hemisphere might play an decisive role (Jung-Beeman, 2005). Hayling Sentence Completion Task requires semantic integration (Kircher, Brammer, Andreu, Williams, & McGuire, 2001) and there is evidence that semantic integration elicits functional MRI signal predominantly in the right-hemisphere (St George, Kutas, Martinez, & Sereno, 1999), and patients with and intact left hemisphere but with a damage in the left hemisphere may miss the main sense of a story – although they do not appear aphasic (Beeman et al., 1994).

In addition, the right hemisphere is thought to play a greater role than the left hemisphere when people are asked to find and produce the "best ending" to a sentence (Kircher, et al., 2001). Therefore, the rightward increased functional connectivity observed in the present study might depend on cross-condition demands of the HSCT.

The HSCT implies also "semantic selection", that is defined as the interactive process by which competing activated concepts are sorted out through the inhibition of competing concepts while selecting one concept for action, including response production. There is evidence that semantic selection depends on the IFG bilaterally (Barch, et al., 1999; Kan & Thompson-Schill, 2004; Miller & Cohen, 2001).

Also Seger (2000) demonstrated that the right IFG is more strongly active than the left homologue when subjects are asked to produce an unusual use of nouns, which might be a process required also in the response Suppression condition of the Hayling, in which participants had to complete the sentence with an incongruent word.

To conclude, it is difficult to draw a firm conclusion based on previous studies since, as I already mentioned, functional connectivity in association with regional activation observed during this task has not been addressed yet.

5. FUNCTIONAL AND STRUCTURAL CONNECTIVITY LATERALISATION WITHIN THE PERISYLVIAN LANGUAGE NETWORK: A COMBININED FMRI AND DTI STUDY

5.1 Introduction

Obtaining a deeper understanding of structure-function relations in the human brain is an important goal of neuroscience.

Structural connectivity measured by the means of DTI has been found to correlate with functional ability across several networks in the brain (Glenn et al., 2007; A. Turken et al., 2008; van Eimeren, Niogi, McCandliss, Holloway, & Ansari, 2008). In addition to structural connectivity, MRI can be used to obtain a measure of functional relationships between brain regions using blood oxygen level dependent functional MRI (fMRI). In fact, the measurement of functional coupling between brain regions using correlations in low frequency fMRI BOLD oscillations reveals functional connectivity between these regions.

So far there have been only a small number of studies that have related these diverse modalities or tried to correlate functional and structural connectivities. In fact, they provide measurements of quite different characteristics of the brain therefore it is still unclear to what degree they may be related.

Aiming to examine this relationship, some studies have independently examined DTI and fMRI data acquired in the same session (Riecker et al., 2007; Seghier et al., 2004) trying to characterize both structural connectivity using DTI and location of fMRI activity in healthy and pathological conditions. The combination of DTI and fMRI

measurements into a single analysis may give unique information not available with either single modality. Conventionally the functional information is used to guide the fiber-tracking by defining functional regions (Dougherty, Ben-Shachar, Bammer, Brewer, & Wandell, 2005; Guye et al., 2003; Johansen-Berg et al., 2005). Although these studies have investigated both fMRI and DTI measures of activity to analyze a single network, only a few reports were found that openly related fMRI functional connectivity and DTI derived structural connectivity in a single network. In one research these measurements were restricted to two adjacent gyri in the frontal lobe with results showing that the relationship between these two modalities is complex (Koch, Norris, & Hund-Georgiadis, 2002). High functional connectivity was found between regions with low structural connectivity, possibly due to fibers not contained within the imaging slice or indirect structural connections; but low functional connectivity was not found between regions with high structural connectivity. In a second study involving patients with multiple sclerosis, structural connectivity measured as FA was found to be positively correlated with functional connectivity only when the controls and patients were combined (Lowe et al., 2008). Skudlarski et al. (2008) looked at functional vs. anatomic connectivity across the whole brain and in anatomically defined regions and found good overall spatial overlap between the two types of connectivity maps. They also found that congruency between the individual measures is increased when the individual measures themselves are increased.

(Vernooij, et al., 2007) were the first to combine fMRI and DTI to investigate the lateralisation of the arcuate fasciculus and the functional hemispheric language lateralisation. They performed functional magnetic resonance imaging fMRI and DTI on 20 healthy volunteers, including 13 left-handers. Although functional

hemispheric language lateralisation was right-sided in five left-handed individuals, the results showed an overall significant leftward asymmetry in the arcuate fasciculus, regardless of handedness or functional language lateralisation. Furthermore, in right-handers, the degree of structural asymmetry was found to be correlated with the degree of functional lateralisation. The authors concluded that white matter asymmetry in the arcuate fasciculus does not seem to reflect functional hemispheric language lateralisation, as had been suggested previously (Lurito & Dzemidzic, 2001; Pujol, et al., 1999), but they suggest that the previously reported white matter asymmetry might be explained by a structural asymmetry in the arcuate fasciculus.

Using DTI for arcuate fasciculus identification, in conjunction with fMRI for determination of functional language lateralisation, another study (Propper, et al., 2010) investigated the relationship between language lateralisation and arcuate fasciculus asymmetry, being the first to examine this relationship as a function of both direction and degree of hand preference using DTI tractography on 9 male and 17 females with different degrees of handedness. An effect of degree of handedness was found on arcuate fasciculus structure, such that consistently-handed individuals, irrespective of the direction of hand preference, demonstrated the most lateralised arcuate fasciculus, with larger left versus right arcuate, as measured by DTI. Functional language lateralisation in Wernicke's area, assessed with fMRI, was correlated to arcuate fasciculus volume exclusively in consistent-left-handers, and only in people who were not right hemisphere lateralised for language.

Another study (Powell, et al., 2006) combined fMRI and diffusion-weighted imaging (DWI) with tractography and employed only right-handed subjects (N=10) to investigate language-related regions in inferior frontal and superior temporal

regions. A probabilistic tractography technique was then employed to delineate the connections of these functionally defined regions. The findings showed connections between Broca's and Wernicke's areas along the superior longitudinal fasciculus bilaterally but more extensive frontotemporal connectivity on the left than the right. In addition both tract volumes and mean fractional anisotropy (FA) were significantly higher on the left than the right. The results displayed also a correlation between measures of structure and function, with subjects with more lateralised fMRI activation having a greater lateralised mean FA of their connections. These structural asymmetries are consistent with the lateralisation of language function.

In this study, our goal was to explore the relationship between structural and functional data. Specifically, DTI structural connectivity indices were compared to fMRI functional connectivity indices between regions activated in a series of language tasks in the left frontal (premotor and Broca's area) and the left parietal temporal region (Wernicke's area) in a population of right-handed, healthy controls. We hypothesize that this analysis will more directly elucidate any linear relationships existing between MRI structural and functional connectivity between functionally activated regions across a network.

5.2 Methods

5.2.1 Participants

Healthy controls. Twenty-two healthy male (n=11) and female (n=11) were recruited by advertisement from the same local community as the ARMS and FEP groups. However, after pre-processing of the fMRI images one of the male volunteers

was removed on the basis of excessive head movements inside the scanner, leaving scans from 22 healthy controls for the subsequent analysis.

	Healthy controls (n = 22)
Age (years)	24.36 (4.3)
Gender	11M:11F
WRAT estimated premorbid IQ	108.95 (9.6)
Years of education	15.59 (2.7)
Antipsychotic	2M:19N
Symptoms	
PANSS total	NA
PANSS positive	NA
PANSS negative	NA
PANSS hallucination	NA
PANSS delusions	NA

Table 5.7. Mean and standard deviation of demographic, neuropsychological and clinical characteristics of the three groups.

5.2.2 fMRI task design and data acquisition

The fMRI paradigm and the fMRI data acquisition procedure are described in detail in Chapter 4, methods section 4.2.

DTI data acquisition procedure and details are reported in Chapter 3, methods section 3.2.4.

5.2.3 fMRI and DTI data analysis

Activation maps were calculated for each subject and used to localise the functionally activated language regions of interest across groups. The preprocessing and standard statistical parametric mapping (SPM) analysis of fMRI data are reported in details in chapter 4, methods section 4.2.4. DTI tractography and virtual dissection of the AF were used to derive mean FA values for the anterior, long and posterior segments of the AF. Details of DTI data preprocessing, tractography and virtual dissection procedure for the arcuate fasciculus and FA statistical analysis are described in Chapter 3, methods section 3.2.5.

5.2.4 Functional connectivity analysis

In the present exploratory study, there were no specific a-priori hypotheses as to the directionality (i.e forward versus backward) of the inter-regional interactions and the impact of the experimental condition on the relationship between structural and functional connectivity within the perisylvian network. Thus an exploratory correlation analysis based on Pearson's correlation coefficient was preferred to a more hypothesis-driven analytical approach (e.g. Dynamic Causal Modelling).

Regions of interest (ROIs) identification. For the purpose of this study, time-series were extracted from three ROIs: the left inferior frontal gyrus (LIFG), the middle temporal gyrus (LMTG) and the left inferior parietal lobule. These regions have been previously implicated in studies investigating language and semantic processing (Price, 2000a, 2010) and represent the perysilvian network of regions connected

through the AF (Catani, et al., 2005). In order to ensure comparability across subjects, the extraction of time series had to meet a combination of anatomical and functional criteria (Stephan et al., 2007). Functionally, the principal eigenvariates were extracted to summarise regional responses in 12 mm spheres centred on the ROIs included in the study. To account for individual differences, the location of these regions was based upon the local maxima of the subject-specific statistical parametric maps, defined as the nearest (within 10 mm) of the group maxima. The mean coordinates for the LIFG and LMTG were derived from activation maps obtained with the standard SPM analysis of the HSC task data. In healthy controls, the group maximum in LMTG was [-58, -40, 2] and in the LIFG was [-40, 22, -6]. The mean coordinates for the LIPL were derived from previous studies which provided evidence of LIPL involvement in semantic processing (Price, 2010) and were defined as [-47, -59, 40]. Anatomically, the search for each subject-specific local maximum was constrained within the same correspondent cortical area, as defined by the PickAtlas toolbox (Maldjian, Laurienti, Kraft, & Burdette, 2003a). There were no regions that conformed to these criteria in one subject, who was therefore excluded from this study. Figure 7.1a shows the PLN and the functional connections investigated in this study.

fMRI inter-regional Pearson's correlation analysis. In this study I aimed to explore the relationship between mean FA values along the three segments of the AF and inter-regional functional coupling between perisylvian brain regions connected through this white matter bundle. For each subject, a Pearson's correlation coefficient was calculated between LIFG and LMTG, LMTG and LIPL and LIFG and LIPL using the time-series extracted from each ROI. Age was entered in each analysis as a covariate of no interest in order to remove the confounding effects of this variable.

5.2.5 Correlation analysis

To assess the relationship between functional and structural connectivity within the PLN, an exploratory correlation analysis was performed between the strength of inter-regional coupling between each pair of regions and the mean FA value of the specific segment of the AF connecting these regions. More specifically, Pearson's correlation coefficients were computed between functional and structural connectivity measures of: (i) LIFG-LIPL and left anterior segment of the AF, (ii) LIFG-LMTG and left long segment of the AF, and (iii) LMTG-LIPL and left posterior segment of the AF. Age might be differentially associated with structural and functional connectivity measures. For instance, there is evidence that normal aging is associated with reduced strength of anatomical connections but with either reduced and increased strength of functional connections (Schlee, Leirer, Kolassa, Weisz, & Elbert, 2012; Stevens, Skudlarski, Pearlson, & Calhoun, 2009). Therefore, an additional partial correlation analysis was performed in which age was defined as variable of no interest to control for the potential confounding effects of this variable. Results are reported for each correlation analysis. Given the exploratory nature of these correlation analyses, statistical significance was set at $p = 0.05$ (two-tailed).

Subsequently, Pearson's correlation coefficients were converted in Z scores by applying a Fischer's transformation and two independent tests were computed to compare left and right Z scores in the anterior and long segment of the arcuate fasciculus.

5.3. Results

5.3.1 fMRI data and standard SPM analysis

Results of the standard SPM analysis are reported in detail in Chapter 4, section 4.3.2. In brief, increased BOLD response across all task conditions compared to Repetition was observed in a fronto-temporal network of regions including the left SFG, the ventro-lateral IFG and lateral MTG bilaterally. (Figure 4.1 to 4.5, Chapter 4).

5.3.2 Functional connectivity analysis within the perisylvian language network

A positive correlation was observed between regional time-series in the LIFG and LIPL, LMTG and LIFG, and LMTG and LIPL (Table 4.2, Chapter 4).

5.3.3 Relationship between functional and structural connectivity

The linear correlation analysis between the DTI-derived structural connectivity and the fMRI-derived functional connectivity within the language network of interest yielded two statistically significant relationships within the group (Table 5.2 to 5.3). More specifically, subject-specific mean FA values in the left long segment of the AF were negatively correlated with subject-specific correlation coefficients between time-series in the LMTG and LIFG (R = -0.452, p = 0.006). In addition, subject-specific mean FA values in the right anterior segment of the AF were negatively correlated with subject-specific correlation coefficients between time-series in the RIFG and RIPL (R = -0.561, p =0.008).

Moreover, when Fischer's transformation was applied to the correlation coefficients and the long and anterior segments were contrasted by the hemispheres specific *Z*-scores no significance difference was detected between left and right correlation coefficients.

No significant correlation between the Lateralisation Index of the FA values in the three segments of the AF and the Lateralisation Index of functional connectivity between the brain regions they are thought to connect were observed (Table 5.4).

		Functional connectivity					
		LIFG_LIPL (anterior)		LIFG_LMTG (long)		LMTG_LIPL (post)	
		R	*p*	r	*p*	r	*p*
Fractional anisotropy	L anterior	-.119	.628	-.452	.052	.010	.969
	L long	-.248	.279	-.452	.006	.-468	.033
	L post	-.178	.439	-.372	.096	-.109	.637

Table 5.8. Correlation analysis between the DTI-derived structural connectivity and the fMRI-derived functional connectivity within the language network in the left hemisphere

		Functional connectivity					
		RIFG_RIPL (anterior)		RIFG_RMTG (long)		RMTG_RIPL (post)	
		R	*p*	r	*p*	r	*p*
Fractional anisotropy	R anterior	-.561	.008	-.214	.352	-.609	.003
	R long	-.432	.057	-.192	.418	-.347	.134

	R post	-.050	.829	.038	.871	.158	.494

Table 5.9. Correlation analysis between the DTI-derived structural connectivity and the fMRI-derived functional connectivity within the language network in the left hemisphere

		LI FC					
		IFG_IPL (anterior)		IFG_MTG (long)		MTG_IPL (post)	
		r	*p*	r	*p*	r	*p*
LI FA	anterior	-.063	.797	-.002	.992	-.183	452
	long	.020	.993	-.323	.165	-.140	.021
	post	-.456	.038	.310	.171	-.316	.162

Table 5.3. Correlation between the Lateralisation Index of the FA values in the three segments of the AF and the Lateralisation Index of functional connectivity between the ROI

5.4 Discussion

The present study combined fMRI and DTI analyses to explore functional and structural connectivity and their relationship within the left perisylvian language network and its homologue in the right hemisphere. The structural connectivity analysis revealed significant leftward asymmetry in the FA values of the long direct segment of the arcuate fasciculus. The functional connectivity analysis revealed that all the correlations between paired ROIs were significantly different from zero and they were all positive. In addition, the lateralisation index calculated from functional connectivity values in all the 3 investigated tracts revealed a rightward lateralisation in the anterior connection, between Broca's and Geschwind's areas. Furthermore, the correlation analysis demonstrated significant negative relations between the mean FA values in the long segment of the AF and the strength of inter-regional

coupling between the IFG and the MTG in the left hemisphere, and between the mean FA values in the anterior segment of the AF and the strength of regional coupling between IFG and IPL in the right hemisphere. Finally, there were no significant correlations between laterality indices estimated on FA and functional connectivity values.

To my knowledge the present study is the first report of an inverse correlation between FA, and fcMRI cc. values.

The counterintuitive negative correlation between FA values in the left long segment of the AF and the subject-specific correlation coefficients between time-series in the LMTG and LIFG detected in the fronto-temporal language pathway may reflect the complex nature of their relationship and depend specifically on the nature of the fMRI task employed in this study. For instance, no significant correlation was found in a previous study that investigated the relationship between functional and structural connectivity between Broca's and Wernicke's area and used resting-state fMRI data for the functional connectivity (Morgan, Mishra, Newton, Gore, & Ding, 2009).

While FA measures can be affected by several microstructural aspects such as myelination, axonal diameter, axon density and relative orientation of axons within the fibre bundle (Papadakis et al., 1999), it is unclear to what degree white matter FA changes are related to brain inter-regional coupling. At present, the exact relationship between variation of microstructural aspects in a specific white matter tract and alterations in functional integration between the regions connected through the same tract is not well established and, therefore, conclusions need to be drawn cautiously and are necessary tentative and speculative. Given that FA measures can be affected by several microstructural aspects of fibre bundles, it is

possible to speculate that low FA values in a specific white matter tract reflect a less efficient interaction between the two brain areas connected through the tract . If that was the case, it might be possible that when this structural “impairment” is present a compensatory reorganisation of functional connectivity in the two brain regions occurs. Moreover, such functional compensation could implicate the involvement of other brain regions or connections which would drive the activity in the former ones and that were not included in the functional connectivity analysis, such as inter-hemispheric connections.

The review of diffusion tractography and functional mapping together highlights the possibility that future strategies for understanding interactions between regions of the human brain will benefit from integrating anatomically informed models of functional interactions.

6. CONCLUSIONS

6.1 Summary of main results

The main aim of the present doctoral work was to better delineate the relationship between anatomical and functional correlates of hemispheric dominance in the perisylvian language network. To this purpose I applied a multi-modal neuroimaging approach including DTI and fMRI on a population of 23 healthy individuals.

A virtual in vivo interactive dissection of the three subcomponents of the arcuate fasciculus was carried out and measures of perisylvian white matter integrity were derived from tract-specific dissection. Consistently with previous studies, the main finding of the present study is a significant leftward asymmetry in the FA value of the long direct segment of the arcuate fasciculus. Greater FA values in the arcuate fasciculus compared with the corresponding white matter tract in the right hemisphere have been reported previous in several studies (Barrick, et al., 2007; Buchel, et al., 2004; Catani, et al., 2007; Powell, et al., 2006). In addition, we found another significant leftward lateralisation in the SL of the posterior segment and a rightward distribution of the SL index of the anterior segment of the arcuate fasciculus. In addition, I found no evidence of a significant relationship between the leftward lateralisation indexes and any measures of language and verbal memory performance in my group.

Subsequently, I implemented functional connectivity analysis to test whether leftward lateralisation of connectivity indexes between perisylvian regions can be observed in individuals performing a language-related task. The main finding of the

fc analysis is a significant rightward lateralisation (left, 0.347 ± 0.183; right, 0.493 ± 0.228; P = 0.037) in the anterior connection, between the the IFG and the IPL. The functional connectivity analysis revealed an increase in the strength of inter-regional coupling between the RIFG and RIPL.

Finally, I combined DTI and fMRI data to examine whether a significant relationship is present between these measures of perisylvian connectivity and it significantly differs between hemispheres.

The correlation analysis demonstrated significant negative relations between the mean FA values in the long segment of the AF and the strength of inter-regional coupling between the IFG and the MTG in the left hemisphere, and between the mean FA values in the anterior segment of the AF and the strength of regional coupling between IFG and IPL in the right hemisphere. Finally, there were no significant correlations between laterality indices estimated on FA and functional connectivity values.

6.2 Implications for neurobiological models of perisylvian connectivity correlates of the hemispheric dominance for language

Three important findings emerge from this study. First, this study confirms that white matter indexes of perisylvian language networks differ between the two hemispheres and that, in addition, the pattern of lateralisation is heterogeneous in the normal population. The overall prevalence of leftward distribution of the direct segment of the arcuate fasciculus (78.3%) is higher than the prevalence of bilateral symmetrical (21.7%) or rightward (0%) distribution in our right-handed sample. Considering that the prevalence of left functional "dominance" for language is 90%

(Toga & Thompson, 2003), leftward lateralisation of the long segment may represent a crucial anatomical correlate for language lateralisation.

To better investigate whether the observed leftward asymmetry of white matter FA value in the long direct segment of the arcuate fasciculus represents a potential anatomical substrate of language lateralisation, I carried out a number of correlation analyses between this measure and measures of language processing abilities, which showed no evidence of such significant associations. This is in line with evidence from previous DTI studies reporting similar findings (Catani, et al., 2007). A possible explanation for the lack of significant correlation is that the language tasks I used in the current work do not depend exclusively on a specific anatomical connection but rely on a more extended network including extra-perisylvian regions. An alternative possibility is that performances on language-related cognitive tasks do not rely solely on measure of integrity of anatomical connection within the perisylvian network.

Secondly, unlike anatomical measures, functional connectivity indeces did not show evidence of an alike leftward asymmetry. Indeed, the strength of functional connections was increased between perisylvian regions in both the left and right hemisphere during the execution of the HSCT task and a significant rightward increase of functional connectivity was observed only in the anterior segment of the arcuate fasciculus. This observation seems to suggest that functional connectivity measures might not represent a stable index of hemispheric dominance for language processing when derived by applying complex linguistic tasks implying the interaction of several language-related processes such as verbal recall, semantic selection and response inhibition. Interestingly, this appears to provide evidence in

support of the recent notion that the right hemisphere might also play an important role in language processing.

Finally, the unexpected negative correlation observed between anatomical and functional connectivity measures in the left direct segment may reflect the complex nature of their relationship and depend specifically on the nature of the fMRI task employed in this study. For example, no significant correlation was found in a previous study that investigated the relationship between functional and structural connectivity between Broca's and Wernicke's areas and used resting-state fMRI data for the functional connectivity (Morgan, et al., 2009). Although beyond the purpose of this work, a possible explanation for the negative direction of this relationship might imply that when a structural "deficiency" is present a compensatory reorganisation of functional connectivity occurs between the two regions connected by the specific subcomponents of the arcuate fasciculus. However, I found no evidence of asymmetrical distribution of the correlation coefficients between the two hemispheres. This observation supports the notion, mentioned above, that whilst structural connectivity measures within the perisylvian network seem to be a consistent correlate of hemispheric dominance for language processing, those measures obtained by applying complex cognitive linguistic tasks might not represent an accurate neuro-correlate of the same hemispheric dominance.

6.3 Strenghts and limitations

The major strength of the present doctoral work is that it employed a multimodal imaging approach to investigate structural and function lateralisation. Compared to single modality studies, this approach allows one to derive structural connectivity

and inter-regional coupling measures within the same sample of participants. Moreover, it permits to examine the relationships of measures derived from different modalities. Finally, since neuroimaging measures were acquired within the same acquisition session the potential confounds associated with the time elapsing between two acquisition sessions were avoided and a more reliable integration of data across multiple imaging modalities was enabled.

In addition, in this doctoral work, I employed a virtual *in vivo* interactive dissection of specific white matter bundles thought to connect frontal and temporal brain regions. Unlike DTI methods that employ VBM or ROI approaches that do not precisely identify the white matter tracts and fail to provide quantitative measurements of tract-specific white matter, by using the virtual *in vivo* interactive tractography I was able to derive specific quantitative measurements of microstructural integrity of the arcuate fasciculus and its subcomponents.

However, it might be argued that the main limitation of the present doctoral work is the small number of participants included. Nevertheless, a recent analysis of effect size in classical inference has demonstrated that in order to optimize the sensitive to large effect while minimizing the risk of detecting trivial effects, the optimum sample size for a study is 16 (K. Friston, 2012).

6.4 Future directions

Although previous neuroimaging studies have – so far – provided a rich body of evidence for structural and functional correlates of hemispheric dominance for language, structural and functional connectivity correlates of the same dominance has been poorly investigated and mostly in independent sample. In addition, the

relationship between language-related anatomical and functional connectivity measures has yet to be elucidated. Therefore, in the future this specific aspect should be investigated by implementing multi-modal imaging approaches and a systematic fashion.

A possible future extension of the present doctoral work would be to apply the same methodological approach to the study of neurological and psychiatric conditions implicating language processing impairments. For instance, chronic schizophrenia presents with psychotic symptoms, such as auditory verbal hallucinations and speech disorganization, which are thought to reflect underlying cognitive and language processing deficits, especially in language production and semantic processing (Frith, 1995). Early studies of language lateralisation in patients with chronic schizophrenia have suggested that schizophrenia symptoms might reflect a disturbance of the mechanism by which the hemisphere dominance of language processing is generated and maintained in schizophrenia (Crow, 1997; Crow et al., 1989).

REFERENCES

Allen, P., Mechelli, A., Stephan, K. E., Day, F., Dalton, J., Williams, S., & McGuire, P. K. (2008). Fronto-temporal interactions during overt verbal initiation and suppression. *J Cogn Neurosci, 20*(9), 1656-1669. doi: 10.1162/jocn.2008.20107

Allen, P., Stephan, K. E., Mechelli, A., Day, F., Ward, N., Dalton, J., . . . McGuire, P. (2010). Cingulate activity and fronto-temporal connectivity in people with prodromal signs of psychosis. *Neuroimage, 49*(1), 947-955. doi: S1053-8119(09)00938-0 [pii]

10.1016/j.neuroimage.2009.08.038

Annett, M. (2002). Non-right-handedness and schizophrenia. [Comment

Letter]. *Br J Psychiatry, 181*, 349-350.

Barch, D. M., Sabb, F. W., Carter, C. S., Braver, T. S., Noll, D. C., & Cohen, J. D. (1999). Overt verbal responding during fMRI scanning: empirical investigations of problems and potential solutions. *Neuroimage, 10*(6), 642-657. doi: 10.1006/nimg.1999.0500

S1053-8119(99)90500-1 [pii]

Barrick, T. R., Lawes, I. N., Mackay, C. E., & Clark, C. A. (2007). White matter pathway asymmetry underlies functional lateralization. [Research Support, Non-U.S. Gov't]. *Cereb Cortex, 17*(3), 591-598. doi: 10.1093/cercor/bhk004

Basser, P. J., Pajevic, S., Pierpaoli, C., Duda, J., & Aldroubi, A. (2000). In vivo fiber tractography using DT-MRI data. *Magn Reson Med, 44*(4), 625-632. doi: 10.1002/1522-2594(200010)44:4<625::AID-MRM17>3.0.CO;2-O [pii]

Basser, P. J., & Pierpaoli, C. (1996). Microstructural and physiological features of tissues elucidated by quantitative-diffusion-tensor MRI. *J Magn Reson B, 111*(3), 209-219.

Beaulieu, C., & Allen, P. S. (1994). Determinants of anisotropic water diffusion in nerves. *Magn Reson Med, 31*(4), 394-400.

Beeman, M., Friedman, R. B., Grafman, J., Perez, E., Diamond, S., & Lindsay, M. B. (1994). Summation Priming and Coarse Semantic Coding in the Right-Hemisphere. *Journal of Cognitive Neuroscience, 6*(1), 26-45.

Behrens, T., Rohr, K., & Stiehl, H. S. (2003). Robust segmentation of tubular structures in 3-D medical images by parametric object detection and tracking. *IEEE Trans Syst Man Cybern B Cybern, 33*(4), 554-561. doi: 10.1109/TSMCB.2003.814305

Bernal, B., & Altman, N. (2010). The connectivity of the superior longitudinal fasciculus: a tractography DTI study. *Magnetic Resonance Imaging, 28*(2), 217-225. doi: DOI 10.1016/j.mri.2009.07.008

Biswal, B., Yetkin, F. Z., Haughton, V. M., & Hyde, J. S. (1995). Functional connectivity in the motor cortex of resting human brain using echo-planar MRI. [Research Support, U.S. Gov't, P.H.S.]. *Magn Reson Med, 34*(4), 537-541.

Bleich-Cohen, M., Sharon, H., Weizman, R., Poyurovsky, M., Faragian, S., & Hendler, T. (2012). Diminished language lateralization in schizophrenia corresponds to impaired inter-hemispheric functional connectivity. *Schizophr Res, 134*(2-3), 131-136. doi: 10.1016/j.schres.2011.10.011

Boatman, D., Gordon, B., Hart, J., Selnes, O., Miglioretti, D., & Lenz, F. (2000). Transcortical sensory aphasia: revisited and revised. *Brain, 123*, 1634-1642.

Broca, P. (1861). Remarques sur le siège de la faculté du language articulé, suivies d'une observation d'aphémie (perte de la parole). . *Bull. Soc. Anthropol., 6*, 330-357.

Brown, R. (1828). A brief account of microscopical observations made in the months of June, July and August 1827 on the particles contained in the pollen of plants; and on the

general existence of active molecules in organic and inorganic bodies. . *Philosophical Magazine, 4*.
Buchel, C., & Friston, K. J. (1997). Modulation of connectivity in visual pathways by attention: cortical interactions evaluated with structural equation modelling and fMRI. *Cereb Cortex, 7*(8), 768-778.
Buchel, C., Raedler, T., Sommer, M., Sach, M., Weiller, C., & Koch, M. A. (2004). White matter asymmetry in the human brain: a diffusion tensor MRI study. [Comparative Study

Research Support, Non-U.S. Gov't]. *Cereb Cortex, 14*(9), 945-951. doi: 10.1093/cercor/bhh055
Burgess, P. W., & Shallice, T. (1996). Response suppression, initiation and strategy use following frontal lobe lesions. *Neuropsychologia, 34*(4), 263-272. doi: 0028-3932(95)00104-2 [pii]
Buxton, R. B., Wong, E. C., & Frank, L. R. (1998). Dynamics of blood flow and oxygenation changes during brain activation: the balloon model. *Magn Reson Med, 39*(6), 855-864.
Cabeza, R., & Nyberg, L. (2000). Imaging cognition II: An empirical review of 275 PET and fMRI studies. [Review]. *J Cogn Neurosci, 12*(1), 1-47.
Catani, M., Allin, M. P., Husain, M., Pugliese, L., Mesulam, M. M., Murray, R. M., & Jones, D. K. (2007). Symmetries in human brain language pathways correlate with verbal recall. [Research Support, Non-U.S. Gov't]. *Proc Natl Acad Sci U S A, 104*(43), 17163-17168. doi: 10.1073/pnas.0702116104
Catani, M., Howard, R. J., Pajevic, S., & Jones, D. K. (2002). Virtual in vivo interactive dissection of white matter fasciculi in the human brain. *Neuroimage, 17*(1), 77-94. doi: S1053811902911365 [pii]
Catani, M., Jones, D. K., & ffytche, D. H. (2005). Perisylvian language networks of the human brain. *Ann Neurol, 57*(1), 8-16. doi: 10.1002/ana.20319
Catani, M., & Thiebaut de Schotten, M. (2008). A diffusion tensor imaging tractography atlas for virtual in vivo dissections. [Research Support, Non-U.S. Gov't]. *Cortex, 44*(8), 1105-1132. doi: 10.1016/j.cortex.2008.05.004
Chenevert, T. L., Brunberg, J. A., & Pipe, J. G. (1990). Anisotropic diffusion in human white matter: demonstration with MR techniques in vivo. *Radiology, 177*(2), 401-405.
Conturo, T. E., Lori, N. F., Cull, T. S., Akbudak, E., Snyder, A. Z., Shimony, J. S., . . . Raichle, M. E. (1999). Tracking neuronal fiber pathways in the living human brain. *Proc Natl Acad Sci U S A, 96*(18), 10422-10427.
Coren, S. (1993a). The Lateral Preference Inventory for Measurement of Handedness, Footedness, Eyedness, and Earedness - Norms for Young-Adults. *Bulletin of the Psychonomic Society, 31*(1), 1-3.
Coren, S. (1993b). Measurement of handedness via self-report: the relationship between brief and extended inventories. *Percept Mot Skills, 76*(3 Pt 1), 1035-1042.
Crawford, J. R., & Henry, J. D. (2003). The Depression Anxiety Stress Scales (DASS): normative data and latent structure in a large non-clinical sample. *Br J Clin Psychol, 42*(Pt 2), 111-131. doi: 10.1348/014466503321903544
Crow, T. J. (1997). Schizophrenia as failure of hemispheric dominance for language. *Trends in Neurosciences, 20*(8), 339-343.
Crow, T. J., Ball, J., Bloom, S. R., Brown, R., Bruton, C. J., Colter, N., . . . Roberts, G. W. (1989). Schizophrenia as an Anomaly of Development of Cerebral Asymmetry - a Postmortem Study and a Proposal Concerning the Genetic-Basis of the Disease. *Archives of General Psychiatry, 46*(12), 1145-1150.
Dale, A. M. (1999). Optimal experimental design for event-related fMRI. *Hum Brain Mapp, 8*(2-3), 109-114. doi: 10.1002/(SICI)1097-0193(1999)8:2/3<109::AID-HBM7>3.0.CO;2-W [pii]
Damasio, A. R., & Geschwind, N. (1984). The Neural Basis of Language. *Annual Review of Neuroscience, 7*, 127-147.

de Groot, M., Vernooij, M. W., Klein, S., Leemans, A., de Boer, R., van der Lugt, A., . . . Niessen, W. J. (2009). Iterative Co-linearity Filtering and Parameterization of Fiber Tracts in the Entire Cingulum. *Medical Image Computing and Computer-Assisted Intervention - Miccai 2009, Pt I, Proceedings, 5761*, 853-860.

Dehaene, S., & Dehaene-Lambertz, G. (2009). [Cognitive neuro-imaging : phylogenesis and ontogenesis]. *Bull Acad Natl Med, 193*(4), 883-889.

Dejerine, J. (1985). *Anatomie des Centre Nerveux.* Rueff et Cie, Paris.

Delis, D. C., Freeland, J., Kramer, J. H., & Kaplan, E. (1988). Integrating clinical assessment with cognitive neuroscience: construct validation of the California Verbal Learning Test. *J Consult Clin Psychol, 56*(1), 123-130.

Desmond, J. E., & Glover, G. H. (2002). Estimating sample size in functional MRI (fMRI) neuroimaging studies: statistical power analyses. *J Neurosci Methods, 118*(2), 115-128. doi: S0165027002001218 [pii]

Doran, M., Hajnal, J. V., Van Bruggen, N., King, M. D., Young, I. R., & Bydder, G. M. (1990). Normal and abnormal white matter tracts shown by MR imaging using directional diffusion weighted sequences. *J Comput Assist Tomogr, 14*(6), 865-873.

Dougherty, R. F., Ben-Shachar, M., Bammer, R., Brewer, A. A., & Wandell, B. A. (2005). Functional organization of human occipital-callosal fiber tracts. *Proc Natl Acad Sci U S A, 102*(20), 7350-7355. doi: 0500003102 [pii]

10.1073/pnas.0500003102

Dronkers, N. F., Wilkins, D. P., Van Valin, R. D., Jr., Redfern, B. B., & Jaeger, J. J. (2004). Lesion analysis of the brain areas involved in language comprehension. [Research Support, U.S. Gov't, Non-P.H.S.

Research Support, U.S. Gov't, P.H.S.

Review]. *Cognition, 92*(1-2), 145-177. doi: 10.1016/j.cognition.2003.11.002

Duffau, H., Gatignol, P., Moritz-Gasser, S., & Mandonnet, E. (2009). Is the left uncinate fasciculus essential for language? *Journal of Neurology, 256*(3), 382-389. doi: DOI 10.1007/s00415-009-0053-9

Fox, M. D., Snyder, A. Z., Vincent, J. L., Corbetta, M., Van Essen, D. C., & Raichle, M. E. (2005). The human brain is intrinsically organized into dynamic, anticorrelated functional networks. *Proc Natl Acad Sci U S A, 102*(27), 9673-9678. doi: DOI 10.1073/pnas.0504136102

Friston, K. (2012). Ten ironic rules for non-statistical reviewers. *Neuroimage, 61*(4), 1300-1310. doi: 10.1016/j.neuroimage.2012.04.018

S1053-8119(12)00399-0 [pii]

Friston, K. J. (1994). Functional and effective connectivity in neuroimaging. *Human Brain Mapping, 2*, 56-78.

Friston, K. J., Frith, C. D., Frackowiak, R. S., & Turner, R. (1995). Characterizing dynamic brain responses with fMRI: a multivariate approach. *Neuroimage, 2*(2), 166-172. doi: S1053811985710191 [pii]

Friston, K. J., Holmes, A., Poline, J. B., Price, C. J., & Frith, C. D. (1996). Detecting activations in PET and fMRI: levels of inference and power. *Neuroimage, 4*(3 Pt 1), 223-235. doi: S1053-8119(96)90074-9 [pii]

10.1006/nimg.1996.0074

Friston, K. J., Holmes, A. P., Poline, J. B., Grasby, P. J., Williams, S. C., Frackowiak, R. S., & Turner, R. (1995). Analysis of fMRI time-series revisited. [Research Support, Non-U.S. Gov't]. *Neuroimage, 2*(1), 45-53. doi: 10.1006/nimg.1995.1007

Friston, K. J., Holmes, A. P., & Worsley, K. J. (1999). How many subjects constitute a study? *Neuroimage, 10*(1), 1-5. doi: 10.1006/nimg.1999.0439

S1053-8119(99)90439-1 [pii]
Frith, C. D. (1995). The cognitive abnormalities underlying the symptomatology and the disability of patients with schizophrenia. *International Clinical Psychopharmacology, 10*, 87-98. doi: Doi 10.1097/00004850-199509003-00012
Frith, C. D., Friston, K. J., Herold, S., Silbersweig, D., Fletcher, P., Cahill, C., . . . Liddle, P. F. (1995). Regional brain activity in chronic schizophrenic patients during the performance of a verbal fluency task. *Br J Psychiatry, 167*(3), 343-349.
Galaburda, A. M., LeMay, M., Kemper, T. L., & Geschwind, N. (1978). Right-left asymmetrics in the brain. [Research Support, U.S. Gov't, Non-P.H.S.

Research Support, U.S. Gov't, P.H.S.

Review]. *Science, 199*(4331), 852-856.
Galantucci, S., Tartaglia, M. C., Wilson, S. M., Henry, M. L., Filippi, M., Agosta, F., . . . Gorno-Tempini, M. L. (2011). White matter damage in primary progressive aphasias: a diffusion tensor tractography study. *Brain, 134*, 3011-3029. doi: Doi 10.1093/Brain/Awr099
Gazzaniga, M. S. (2000). Cerebral specialization and interhemispheric communication: does the corpus callosum enable the human condition? [Research Support, Non-U.S. Gov't

Research Support, U.S. Gov't, P.H.S.

Review]. *Brain, 123 (Pt 7)*, 1293-1326.
Geschwin.N, & Levitsky, W. (1968). Human Brain - Left-Right Asymmetries in Temporal Speech Region. *Science, 161*(3837), 186-&.
Geschwind, N., & Galaburda, A. M. (1985). Cerebral lateralization. Biological mechanisms, associations, and pathology: I. A hypothesis and a program for research. [Research Support, Non-U.S. Gov't

Research Support, U.S. Gov't, Non-P.H.S.

Research Support, U.S. Gov't, P.H.S.]. *Arch Neurol, 42*(5), 428-459.
Glasser, M. F., & Rilling, J. K. (2008). DTI Tractography of the Human Brain's Language Pathways. *Cerebral Cortex, 18*(11), 2471-2482. doi: DOI 10.1093/cercor/bhn011
Glenn, O. A., Ludeman, N. A., Berman, J. I., Wu, Y. W., Lu, Y., Bartha, A. I., . . . Henry, R. G. (2007). Diffusion tensor MR imaging tractography of the pyramidal tracts correlates with clinical motor function in children with congenital hemiparesis. *AJNR Am J Neuroradiol, 28*(9), 1796-1802. doi: ajnr.A0676 [pii]

10.3174/ajnr.A0676
Goense, J. B., & Logothetis, N. K. (2008). Neurophysiology of the BOLD fMRI signal in awake monkeys. *Curr Biol, 18*(9), 631-640. doi: S0960-9822(08)00442-9 [pii]

10.1016/j.cub.2008.03.054
Gong, G. L., Jiang, T. Z., Zhu, C. Z., Zang, Y. F., Wang, F., Xie, S., . . . Gu, X. M. (2005). Asymmetry analysis of cingulum based on scale-invariant parameterization by diffusion tensor imaging. *Human Brain Mapping, 24*(2), 92-98. doi: Doi 10.1002/Hbm.20072
Guye, M., Parker, G. J., Symms, M., Boulby, P., Wheeler-Kingshott, C. A., Salek-Haddadi, A., . . . Duncan, J. S. (2003). Combined functional MRI and tractography to demonstrate the connectivity of the human primary motor cortex in vivo. *Neuroimage, 19*(4), 1349-1360. doi: S1053811903001654 [pii]
Hagmann, P., Cammoun, L., Martuzzi, R., Maeder, P., Clarke, S., Thiran, J. P., & Meuli, R. (2006). Hand preference and sex shape the architecture of language networks. [Comparative Study

Research Support, Non-U.S. Gov't]. *Human Brain Mapping, 27*(10), 828-835. doi: 10.1002/hbm.20224
Hickok, G., & Poeppel, I. D. (2000). Towards a functional neuroanatomy of speech perception. *J Cogn Neurosci*, 45-45.
Johansen-Berg, H., Behrens, T. E., Sillery, E., Ciccarelli, O., Thompson, A. J., Smith, S. M., & Matthews, P. M. (2005). Functional-anatomical validation and individual variation of diffusion tractography-based segmentation of the human thalamus. *Cereb Cortex, 15*(1), 31-39. doi: 10.1093/cercor/bhh105

bhh105 [pii]
Johnstone, B., Callahan, C. D., Kapila, C. J., & Bouman, D. E. (1996). The comparability of the WRAT-R reading test and NAART as estimates of premorbid intelligence in neurologically impaired patients. *Arch Clin Neuropsychol, 11*(6), 513-519. doi: 0887-6177(96)82330-4 [pii]
Jones, D. K. (2003). Determining and visualizing uncertainty in estimates of fiber orientation from diffusion tensor MRI. [Research Support, Non-U.S. Gov't]. *Magn Reson Med, 49*(1), 7-12. doi: 10.1002/mrm.10331
Jones, D. K. (2008). Studying connections in the living human brain with diffusion MRI. *Cortex, 44*(8), 936-952. doi: S0010-9452(08)00110-X [pii]

10.1016/j.cortex.2008.05.002
Jones, D. K., & Basser, P. J. (2004). "Squashing peanuts and smashing pumpkins": how noise distorts diffusion-weighted MR data. *Magn Reson Med, 52*(5), 979-993. doi: 10.1002/mrm.20283
Jung-Beeman, M. (2005). Bilateral brain processes for comprehending natural language. *Trends Cogn Sci, 9*(11), 512-518. doi: S1364-6613(05)00271-8 [pii]

10.1016/j.tics.2005.09.009
Kaas, J. H., & Hackett, T. A. (1999). 'What' and 'where' processing in auditory cortex. *Nature Neuroscience, 2*(12), 1045-1047.
Kan, I. P., & Thompson-Schill, S. L. (2004). Selection from perceptual and conceptual representations. *Cogn Affect Behav Neurosci, 4*(4), 466-482.
Kang, X. J., Herron, T. J., & Woods, D. L. (2011). Regional variation, hemispheric asymmetries and gender differences in pericortical white matter. *Neuroimage, 56*(4), 2011-2023. doi: DOI 10.1016/j.neuroimage.2011.03.016
Kircher, T. T. J., Brammer, M., Andreu, N. T., Williams, S. C. R., & McGuire, P. K. (2001). Engagement of right temporal cortex during processing of linguistic context. *Neuropsychologia, 39*(8), 798-809.
Koch, M. A., Norris, D. G., & Hund-Georgiadis, M. (2002). An investigation of functional and anatomical connectivity using magnetic resonance imaging. *Neuroimage, 16*(1), 241-250. doi: 10.1006/nimg.2001.1052

S1053811901910523 [pii]
Lawrie, S. M., Buechel, C., Whalley, H. C., Frith, C. D., Friston, K. J., & Johnstone, E. C. (2002). Reduced frontotemporal functional connectivity in schizophrenia associated with auditory hallucinations. *Biol Psychiatry, 51*(12), 1008-1011. doi: S0006322302013161 [pii]
Le Bihan, D. (2003). Looking into the functional architecture of the brain with diffusion MRI. *Nat Rev Neurosci., 4*(6), 469-480.
Lezak, M. D., Howieson, D. B., & Loring, D. B. (2004). *Neuropsychological Assessment*. Oxford.
Liu, H., Stufflebeam, S. M., Sepulcre, J., Hedden, T., & Buckner, R. L. (2009). Evidence from intrinsic activity that asymmetry of the human brain is controlled by multiple factors. [Research Support, N.I.H., Extramural

Research Support, Non-U.S. Gov't]. *Proc Natl Acad Sci U S A, 106*(48), 20499-20503. doi: 10.1073/pnas.0908073106
Liu, Y., Metens, T., Absil, J., De Maertelaer, V., Baleriaux, D., David, P., . . . Aeby, A. (2011). Gender Differences in Language and Motor-Related Fibers in a Population of Healthy Preterm Neonates at Term-Equivalent Age: A Diffusion Tensor and Probabilistic Tractography Study. *American Journal of Neuroradiology, 32*(11), 2011-2016. doi: Doi 10.3174/Ajnr.A2690
Logothetis, N. K., & Pfeuffer, J. (2004). On the nature of the BOLD fMRI contrast mechanism. *Magn Reson Imaging, 22*(10), 1517-1531. doi: S0730-725X(04)00301-7 [pii]

10.1016/j.mri.2004.10.018
Loonstra, A. S., Tarlow, A. R., & Sellers, A. H. (2001). COWAT metanorms across age, education, and gender. *Appl Neuropsychol, 8*(3), 161-166. doi: 10.1207/S15324826AN0803_5
Lowe, M. J., Beall, E. B., Sakaie, K. E., Koenig, K. A., Stone, L., Marrie, R. A., & Phillips, M. D. (2008). Resting state sensorimotor functional connectivity in multiple sclerosis inversely correlates with transcallosal motor pathway transverse diffusivity. *Hum Brain Mapp, 29*(7), 818-827. doi: 10.1002/hbm.20576
Ludwig, E., & Klinger, J. (1956). *Atlas Cerebri Humani*. Karger, Basel.
Lurito, J. T., & Dzemidzic, M. (2001). Determination of cerebral hemisphere language dominance with functional magnetic resonance imaging. [Review]. *Neuroimaging Clin N Am, 11*(2), 355-363, x.
Magistretti, P. J., & Pellerin, L. (1999). Cellular mechanisms of brain energy metabolism and their relevance to functional brain imaging. *Philos Trans R Soc Lond B Biol Sci, 354*(1387), 1155-1163. doi: 10.1098/rstb.1999.0471
Maldjian, J. A., Laurienti, P. J., Kraft, R. A., & Burdette, J. H. (2003a). An automated method for neuroanatomic and cytoarchitectonic atlas-based interrogation of fMRI data sets. *Neuroimage, 19*(3), 1233-1239. doi: S1053811903001691 [pii]
Maldjian, J. A., Laurienti, P. J., Kraft, R. A., & Burdette, J. H. (2003b). An automated method for neuroanatomic and cytoarchitectonic atlas-based interrogation of fMRI data sets. *Neuroimage, 19*(3), 1233-1239. doi: Doi 10.1016/S1053-8119(03)00169-1
Malykhin, N., Concha, L., Seres, P., Beaulieu, C., & Coupland, N. J. (2008). Diffusion tensor imaging tractography and reliability analysis for limbic and paralimbic white matter tracts. *Psychiatry Research-Neuroimaging, 164*(2), 132-142. doi: DOI 10.1016/j.pscychresns.2007.11.007
Mesulam, M. (2005). Imaging connectivity in the human cerebral cortex: the next frontier? [Comment

Editorial]. *Ann Neurol, 57*(1), 5-7. doi: 10.1002/ana.20368
Mesulam, M. M. (1990). Large-scale neurocognitive networks and distributed processing for attention, language, and memory. [Research Support, Non-U.S. Gov't

Review]. *Ann Neurol, 28*(5), 597-613. doi: 10.1002/ana.410280502
Miller, E. K., & Cohen, J. D. (2001). An integrative theory of prefrontal cortex function. *Annu Rev Neurosci, 24*, 167-202. doi: 10.1146/annurev.neuro.24.1.167

24/1/167 [pii]
Morgan, V. L., Mishra, A., Newton, A. T., Gore, J. C., & Ding, Z. (2009). Integrating functional and diffusion magnetic resonance imaging for analysis of structure-function relationship in the human language network. *PLoS One, 4*(8), e6660. doi: 10.1371/journal.pone.0006660
Mori, S., & Barker, P. B. (1999). Diffusion magnetic resonance imaging: its principle and applications. *Anat Rec, 257*(3), 102-109. doi: 10.1002/(SICI)1097-0185(19990615)257:3<102::AID-AR7>3.0.CO;2-6 [pii]

Mori, S., & van Zijl, P. C. (2002). Fiber tracking: principles and strategies - a technical review. *NMR Biomed, 15*(7-8), 468-480. doi: 10.1002/nbm.781
Mumford, J. A., & Nichols, T. E. (2008). Power calculation for group fMRI studies accounting for arbitrary design and temporal autocorrelation. *Neuroimage, 39*(1), 261-268. doi: S1053-8119(07)00710-0 [pii]

10.1016/j.neuroimage.2007.07.061
Nathaniel-James, D. A., Fletcher, P., & Frith, C. D. (1997). The functional anatomy of verbal initiation and suppression using the Hayling Test. *Neuropsychologia, 35*(4), 559-566. doi: S0028-3932(96)00104-2 [pii]
Nathaniel-James, D. A., & Frith, C. D. (1996). Confabulation in schizophrenia: evidence of a new form? *Psychol Med, 26*(2), 391-399.
Nathaniel-James, D. A., & Frith, C. D. (2002). The role of the dorsolateral prefrontal cortex: evidence from the effects of contextual constraint in a sentence completion task. *Neuroimage, 16*(4), 1094-1102. doi: S1053811902911675 [pii]
Nucifora, P. G., Verma, R., Melhem, E. R., Gur, R. E., & Gur, R. C. (2005). Leftward asymmetry in relative fiber density of the arcuate fasciculus. [Comparative Study

Research Support, N.I.H., Extramural

Research Support, Non-U.S. Gov't

Research Support, U.S. Gov't, P.H.S.]. *Neuroreport, 16*(8), 791-794.
Ogawa, S., Lee, T. M., Kay, A. R., & Tank, D. W. (1990). Brain magnetic resonance imaging with contrast dependent on blood oxygenation. *Proc Natl Acad Sci U S A, 87*(24), 9868-9872.
Ogawa, S., Menon, R. S., Tank, D. W., Kim, S. G., Merkle, H., Ellermann, J. M., & Ugurbil, K. (1993). Functional brain mapping by blood oxygenation level-dependent contrast magnetic resonance imaging. A comparison of signal characteristics with a biophysical model. *Biophys J, 64*(3), 803-812. doi: S0006-3495(93)81441-3 [pii]

10.1016/S0006-3495(93)81441-3
Pajevic, S., Aldroubi, A., & Basser, P. J. (2002). A continuous tensor field approximation of discrete DT-MRI data for extracting microstructural and architectural features of tissue. *J Magn Reson, 154*(1), 85-100. doi: 10.1006/jmre.2001.2452
Pajevic, S., & Pierpaoli, C. (1999). Color schemes to represent the orientation of anisotropic tissues from diffusion tensor data: application to white matter fiber tract mapping in the human brain. *Magn Reson Med, 42*(3), 526-540. doi: 10.1002/(SICI)1522-2594(199909)42:3<526::AID-MRM15>3.0.CO;2-J [pii]
Papadakis, N. G., Xing, D., Houston, G. C., Smith, J. M., Smith, M. I., James, M. F., . . . Carpenter, T. A. (1999). A study of rotationally invariant and symmetric indices of diffusion anisotropy. *Magn Reson Imaging, 17*(6), 881-892. doi: S0730-725X(99)00029-6 [pii]
Papagno, C. (2011). Naming and the Role of the Uncinate Fasciculus in Language Function. *Current Neurology and Neuroscience Reports, 11*(6), 553-559. doi: DOI 10.1007/s11910-011-0219-6
Parker, G. J., Haroon, H. A., & Wheeler-Kingshott, C. A. (2003). A framework for a streamline-based probabilistic index of connectivity (PICo) using a structural interpretation of MRI diffusion measurements. *J Magn Reson Imaging, 18*(2), 242-254. doi: 10.1002/jmri.10350
Parker, G. J., Luzzi, S., Alexander, D. C., Wheeler-Kingshott, C. A., Ciccarelli, O., & Lambon Ralph, M. A. (2005). Lateralization of ventral and dorsal auditory-language pathways in the human brain. [Clinical Trial

Research Support, Non-U.S. Gov't]. *Neuroimage, 24*(3), 656-666. doi: 10.1016/j.neuroimage.2004.08.047

Pauling, L., & Coryell, C. D. (1936). The Magnetic Properties and Structure of Hemoglobin, Oxyhemoglobin and Carbonmonoxyhemoglobin. *Proc Natl Acad Sci U S A, 22*(4), 210-216.
Pierpaoli, C., Jezzard, P., Basser, P. J., Barnett, A., & Di Chiro, G. (1996). Diffusion tensor MR imaging of the human brain. *Radiology, 201*(3), 637-648.
Powell, H. W. R., Parker, G. J. M., Alexander, D. C., Symms, M. R., Boulby, P. A., Wheeler-Kingshott, C. A. M., . . . Duncan, J. S. (2006). Hemispheric asymmetries in language-related pathways: A combined functional MPI and tractography study. *Neuroimage, 32*(1), 388-399. doi: DOI 10.1016/j.neuroimage.2006.03.011
Pravata, E., Sestieri, C., Mantini, D., Briganti, C., Colicchio, G., Marra, C., . . . Caulo, M. (2011). Functional connectivity MR imaging of the language network in patients with drug-resistant epilepsy. *AJNR Am J Neuroradiol, 32*(3), 532-540. doi: 10.3174/ajnr.A2311
Price, C. J. (2000a). The anatomy of language: contributions from functional neuroimaging. *J Anat, 197 Pt 3*, 335-359.
Price, C. J. (2000b). The anatomy of language: contributions from functional neuroimaging. [Research Support, Non-U.S. Gov't

Review]. *Journal of Anatomy, 197 Pt 3*, 335-359.
Price, C. J. (2010). The anatomy of language: a review of 100 fMRI studies published in 2009. *Ann N Y Acad Sci, 1191*, 62-88. doi: NYAS5444 [pii]

10.1111/j.1749-6632.2010.05444.x
Propper, R. E., O'Donnell, L. J., Whalen, S., Tie, Y. M., Norton, I. H., Suarez, R. O., . . . Golby, A. J. (2010). A combined fMRI and DTI examination of functional language lateralization and arcuate fasciculus structure: Effects of degree versus direction of hand preference. *Brain and Cognition, 73*(2), 85-92. doi: DOI 10.1016/j.bandc.2010.03.004
Pujol, J., Deus, J., Losilla, J. M., & Capdevila, A. (1999). Cerebral lateralization of language in normal left-handed people studied by functional MRI. *Neurology, 52*(5), 1038-1043.
Rauschecker, J. P. (1998). Cortical processing of complex sounds. *Curr Opin Neurobiol, 8*(4), 516-521.
Reynolds, C. R. (1984). Wide Range Achievement Test (WRAT-R), 1984 Edition. *Journal of Counseling & Development, 64*(8), 540-541.
Riecker, A., Ackermann, H., Schmitz, B., Kassubek, J., Herrnberger, B., & Steinbrink, C. (2007). Bilateral language function in callosal agenesis: an fMRI and DTI study. *J Neurol, 254*(4), 528-530. doi: 10.1007/s00415-006-0152-9
Romanski, L. M., Tian, B., Fritz, J., Mishkin, M., Goldman-Rakic, P. S., & Rauschecker, J. P. (1999). Dual streams of auditory afferents target multiple domains in the primate prefrontal cortex. *Nature Neuroscience, 2*(12), 1131-1136.
Rubino, C. A. (1970). Hemispheric lateralization of visual perception. *Cortex, 6*(1), 102-120.
Schiff, H. B., Alexander, M. P., Naeser, M. A., & Galaburda, A. M. (1983). Aphemia - Clinical-Anatomic Correlations. *Arch Neurol, 40*(12), 720-727.
Schlee, W., Leirer, V., Kolassa, I. T., Weisz, N., & Elbert, T. (2012). Age-related changes in neural functional connectivity and its behavioral relevance. *BMC Neurosci, 13*, 16. doi: 1471-2202-13-16 [pii]

10.1186/1471-2202-13-16
Scott, S. K., Blank, C. C., Rosen, S., & Wise, R. J. S. (2000). Identification of a pathway for intelligible speech in the left temporal lobe. *Brain, 123*, 2400-2406.
Seger, C. A., Desmond, J. E., Glover, G. H., & Gabrieli, J. D. E. (2000). Functional magnetic resonance imaging evidence for right-hemisphere involvement in processing unusual semantic relationships. *Neuropsychology, 14*(3), 361-369. doi: Doi 10.1037//0894-4105.14.3.361

Seghier, M. L., Lazeyras, F., Zimine, S., Maier, S. E., Hanquinet, S., Delavelle, J., . . . Huppi, P. S. (2004). Combination of event-related fMRI and diffusion tensor imaging in an infant with perinatal stroke. *Neuroimage, 21*(1), 463-472. doi: S1053811903005640 [pii]
Seghier, M. L., & Price, C. J. (2010). Reading Aloud Boosts Connectivity through the Putamen. *Cerebral Cortex, 20*(3), 570-582. doi: DOI 10.1093/cercor/bhp123
Skudlarski, P., Jagannathan, K., Calhoun, V. D., Hampson, M., Skudlarska, B. A., & Pearlson, G. (2008). Measuring brain connectivity: diffusion tensor imaging validates resting state temporal correlations. *Neuroimage, 43*(3), 554-561. doi: 10.1016/j.neuroimage.2008.07.063

S1053-8119(08)00891-4 [pii]
St George, M., Kutas, M., Martinez, A., & Sereno, M. I. (1999). Semantic integration in reading: engagement of the right hemisphere during discourse processing. *Brain, 122 (Pt 7)*, 1317-1325.
Stejskal, E. O., & Tanner, J. E. (1965). Spin diffusion measurements: spin echoes in the presence of a time-dependent field gradient. . *Journal of Chemical Physics, 42*, 288-292.
Stephan, K. E., Harrison, L. M., Kiebel, S. J., David, O., Penny, W. D., & Friston, K. J. (2007). Dynamic causal models of neural system dynamics:current state and future extensions. *J Biosci, 32*(1), 129-144.
Stevens, M. C., Skudlarski, P., Pearlson, G. D., & Calhoun, V. D. (2009). Age-related cognitive gains are mediated by the effects of white matter development on brain network integration. *Neuroimage, 48*(4), 738-746. doi: S1053-8119(09)00706-X [pii]

10.1016/j.neuroimage.2009.06.065
Toga, A. W., & Thompson, P. M. (2003). Mapping brain asymmetry. *Nature Reviews Neuroscience, 4*(1), 37-48. doi: Doi 10.1038/Nrn1009
Tomasi, D., & Volkow, N. D. (2012). Resting functional connectivity of language networks: characterization and reproducibility. *Mol Psychiatry*. doi: 10.1038/mp.2011.177
Turken, A., Whitfield-Gabrieli, S., Bammer, R., Baldo, J. V., Dronkers, N. F., & Gabrieli, J. D. (2008). Cognitive processing speed and the structure of white matter pathways: convergent evidence from normal variation and lesion studies. *Neuroimage, 42*(2), 1032-1044. doi: 10.1016/j.neuroimage.2008.03.057

S1053-8119(08)00286-3 [pii]
Turken, A. U., & Dronkers, N. F. (2011). The neural architecture of the language comprehension network: converging evidence from lesion and connectivity analyses. *Front Syst Neurosci, 5*, 1. doi: 10.3389/fnsys.2011.00001
Upadhyay, J., Hallock, K., Ducros, M., Kim, D. S., & Ronen, I. (2008). Diffusion tensor spectroscopy and imaging of the arcuate fasciculus. [Research Support, N.I.H., Extramural]. *Neuroimage, 39*(1), 1-9. doi: 10.1016/j.neuroimage.2007.08.046
van Atteveldt, N., Roebroeck, A., & Goebel, R. (2009). Interaction of speech and script in human auditory cortex: Insights from neuro-imaging and effective connectivity. *Hearing Research, 258*(1-2), 152-164. doi: DOI 10.1016/j.heares.2009.05.007
van Eimeren, L., Niogi, S. N., McCandliss, B. D., Holloway, I. D., & Ansari, D. (2008). White matter microstructures underlying mathematical abilities in children. *Neuroreport, 19*(11), 1117-1121. doi: 10.1097/WNR.0b013e328307f5c1

00001756-200807160-00007 [pii]
Vanzetta, I., & Grinvald, A. (2001). Evidence and lack of evidence for the initial dip in the anesthetized rat: implications for human functional brain imaging. *Neuroimage, 13*(6 Pt 1), 959-967. doi: 10.1006/nimg.2001.0843

S1053-8119(01)90843-2 [pii]

Vernooij, M. W., Smits, M., Wielopolski, P. A., Houston, G. C., Krestin, G. P., & van der Lugt, A. (2007). Fiber density asymmetry of the arcuate fasciculus in relation to functional hemispheric language lateralization in both right- and left-handed healthy subjects: a combined fMRI and DTI study. *Neuroimage, 35*(3), 1064-1076. doi: 10.1016/j.neuroimage.2006.12.041

Viswanathan, A., & Freeman, R. D. (2007). Neurometabolic coupling in cerebral cortex reflects synaptic more than spiking activity. *Nat Neurosci, 10*(10), 1308-1312. doi: nn1977 [pii]

10.1038/nn1977

Wakana, S., Caprihan, A., Panzenboeck, M. M., Fallon, J. H., Perry, M., Gollub, R. L., . . . Mori, S. (2007). Reproducibility of quantitative tractography methods applied to cerebral white matter. *Neuroimage, 36*(3), 630-644. doi: DOI 10.1016/j.neuroimage.2007.02.049

Wernicke, C. (1874). Der aphasische symptomenkomplex: eine psychologische Studie auf anayomischer Basis

Worsley, K. J., Marrett, S., Neelin, P., Vandal, A. C., Friston, K. J., & Evans, A. C. (1996). A unified statistical approach for determining significant signals in images of cerebral activation. *Hum Brain Mapp, 4*(1), 58-73. doi: 10.1002/(SICI)1097-0193(1996)4:1<58::AID-HBM4>3.0.CO;2-O

Xiang, H. D., Fonteijn, H. M., Norris, D. G., & Hagoort, P. (2010). Topographical functional connectivity pattern in the perisylvian language networks. [Research Support, Non-U.S. Gov't]. *Cereb Cortex, 20*(3), 549-560. doi: 10.1093/cercor/bhp119

Yasmin, H., Aoki, S., Abe, O., Nakata, Y., Hayashi, N., Masutani, Y., . . . Ohtomo, K. (2009). Tract-specific analysis of white matter pathways in healthy subjects: a pilot study using diffusion tensor MRI. *Neuroradiology, 51*(12), 831-840. doi: DOI 10.1007/s00234-009-0580-1

Zarahn, E., Aguirre, G., & D'Esposito, M. (1997). A trial-based experimental design for fMRI. *Neuroimage, 6*(2), 122-138. doi: S1053-8119(97)90279-2 [pii]

10.1006/nimg.1997.0279